PHYSICAL REVIEW D **96,** 063514 (2017)

Cosmological $\mathcal{CP}$-odd axion field as the coherent Berry's phase of the Universe

Shuailiang Ge, Xunyu Liang, and Ariel Zhitnitsky

Department of Physics and Astronomy, University of British Columbia, Vancouver V6T 1Z1, Canada
(Received 9 March 2017; revised manuscript received 9 August 2017; published 14 September 2017)

We consider a dark matter model offering a very natural explanation of the observed relation, $\Omega_{\rm dark} \sim \Omega_{\rm visible}$. This generic consequence of the model is a result of the common origin of both types of matter (dark and visible) which are formed during the same QCD transition. The masses of both types of matter in this framework are proportional to one and the same dimensional parameter of the system, $\Lambda_{\rm QCD}$. The focus of the present work is the detailed study of the dynamics of the $\mathcal{CP}$-odd coherent axion field $a(x)$ just before the QCD transition. We argue that the baryon charge separation effect on the largest possible scales inevitably occurs as a result of merely the existence of the coherent axion field in the early Universe. It leads to preferential formation of one species of nuggets on the scales of the visible Universe where the axion field $a(x)$ is coherent. A natural outcome of this preferential evolution is that only one type of the visible baryons remains in the system after the nuggets complete their formation. This represents a specific mechanism of how the baryon charge separation mechanism (when the Universe is neutral, but the visible part of matter consists of the baryons only) replaces the conventional "baryogenesis" scenario.

DOI: 10.1103/PhysRevD.96.063514

I. INTRODUCTION

The nature of dark matter (DM) and the asymmetry between matter and antimatter are generally assumed to be two unrelated open questions in cosmology. However, we advocate a model, originally suggested in Refs. [1,2], that these two fundamental, naively unrelated, questions are, in fact, closely interconnected. In this model, the matter-antimatter asymmetry (the so-called baryogenesis) is just a $\mathcal{CP}$-violating charge separation process which occurs as a result of a coherent $\mathcal{CP}$-odd axion field over the whole Universe. The unobserved antibaryons in this framework come to comprise the DM in the form of the dense heavy nuggets, similar to Witten's strangelets [3].

This work is the continuation of our previous studies [4] with the main focus on the evolution of a single nugget. A related but distinct question on the global $\mathcal{CP}$-violating separation of baryonic charge was mentioned in Ref. [4] without any quantitative computations.

The main goal of the present work is to present robust arguments (supported by the detail analytical and numerical computations) that a sufficiently strong global $\mathcal{CP}$ violation in form of the fundamental axion field $\theta(x)$ inevitably leads to such a separation of baryon charges. This phenomenon of separation precedes the QCD transition.[1] As we argue in the present work, this axion $\theta(x)$ field can be thought of as Berry's phase, which is coherently accumulated on the largest possible scales of the visible Universe. Precisely this coherence leads to a preferential evolution of the nuggets when one type of visible baryons (not antibaryons) prevails in the system. This source of strong $\mathcal{CP}$ violation is no longer available at the present epoch as a result of the axion dynamics; see the original papers [6–8], recent reviews [9–16], and recent results/proposals on the axion search experiments [17–29].

The basic consequence of this framework is that the visible and dark matter densities are of the same order of magnitude [4]:

$$\Omega_{\rm dark} \approx \Omega_{\rm visible}. \tag{1}$$

This is a very generic consequence of the entire framework, and it is not sensitive[2] to the parameters of the system, such as the axion mass m_a. In our framework, the relation (1) emerges in a very natural way because both types of matter (visible and dark) are proportional to a single dimensional parameter of the system, $\Lambda_{\rm QCD}$.

The very generic relation (1) of this framework is also not sensitive to the initial value θ_0 of the coherent axion field when it starts to oscillate. This should be contrasted with conventional mechanisms (such as production of the axions due to the misalignment mechanism or due to the

[1]It is known that the QCD transition is actually a crossover rather than a phase transition [5] at $\theta = 0$. At a nonvanishing $\theta \neq 0$, the phase diagram is not known. However, in context of the present paper, the important factor is the scale $T_c \sim 170$ MeV where transition happens rather than its precise nature. This region on the QCD phase diagram is denoted by blue dashed line in the vicinity of T_c shown in Fig. 1.

[2]The axion's mass $m_a(T)$ as a function of the temperature at $T > T_c$ has been computed using the lattice simulations by different groups [30–33] with somewhat contradicting results. As we argue in Sec. IV, our main claim (1) is insensitive to a precise value of the axion mass m_a.

domain-wall network decay) which are highly sensitive to these parameters as $\Omega_{\rm axion} \sim \theta_0^2 m_a^{-7/6}$; see reviews [9–16].

In particular, the observed ratio $\Omega_{\rm dark} \simeq 5 \cdot \Omega_{\rm visible}$ would correspond to a slight asymmetric excess of antinuggets compared to the nuggets by a factor of $\sim$0.5 at the end of the nugget's formation, if one assumes that the nuggets saturate the dark matter density today. Thus, the approximate observed ratio $\Omega_{\rm dark} \simeq 5 \cdot \Omega_{\rm visible}$ roughly corresponds to

$$|B_{\rm visible}| : |B_{\rm nuggets}| : |B_{\rm antinuggets}| \simeq 1:2:3, \qquad (2)$$

such that the net baryonic charge is zero.

The quark nuggets at zero temperature satisfy the main criteria to be the DM candidates as they are absolutely stable configurations made of quarks and gluons surrounded by the axion domain wall as described in the original paper [1]. However, unlike conventional dark matter candidates, such as weakly interacting massive particles (WIMPs), the dark-matter/antimatter nuggets are macroscopically large objects, and they strongly interact with visible matter. The quark nuggets do not contradict the observational constraints on dark matter or antimatter for three main reasons [34]:

(i) They carry very large baryon charge $|B| \gtrsim 10^{25}$, and so their number density is very small $\sim B^{-1}$. As a result of this unique feature, their interaction with visible matter is highly inefficient, and therefore the nuggets perfectly qualify as DM candidates. In particular, the quark nuggets essentially decouple from Cosmic Microwave Background (CMB) photons, and therefore they do not destroy the conventional picture for the structure formation.

(ii) The core of the nuggets have nuclear densities. Therefore, the relevant effective interaction is very small $\sigma/M \sim 10^{-10}$ cm^2/g. Numerically, it is comparable with conventional WIMPs values. Therefore, it is consistent with the typical astrophysical and cosmological constraints which are normally represented as $\sigma/M < 1$ cm^2/g.

(iii) The quark nuggets have very large binding energy due to the large gap $\Delta \sim 100$ MeV in superconducting phases. Therefore, the baryon charge is so strongly bounded in the core of the nugget that it is not available to participate in big bang nucleosynthesis at $T \approx 1$ MeV, long after the nuggets had been formed.

We emphasize that the weakness of the visible-dark matter interaction in this model is due to a small geometrical parameter $\sigma/M \sim B^{-1/3}$ which replaces the conventional requirement of sufficiently weak interactions for WIMPs.

We conclude this Introduction with the following remark. We consider the model which has a single fundamental parameter (the mean baryon number of a nugget $\langle B \rangle \sim 10^{25}$, corresponding to the axion mass $m_a \simeq 10^{-4}$ eV). It has been shown that this model is consistent with all known observations, including the satellite and ground-based constraints. It has been also shown that there is a number of frequency bands where some excess of emission was observed, and this model may explain some portion or even the entire excess of the observed radiation in these frequency bands. We refer to the recent short review [35] with a large number of references on original computations which have been carried out for each specific frequency band where some excess of radiation has been observed.

The paper is organized as follows. In Sec. II, we overview the big picture of our framework when the "baryogenesis" is replaced by the baryon charge separation scenario, and the DM is represented by quark nuggets and antinuggets. We list the crucial ingredients of the entire framework by paying special attention to the role the coherent $\mathcal{CP}$-odd axion field discussed in details in Sec. II E.

Essentially, the main objective of the present work is to elaborate on this specific key element of the proposal which has not received sufficient attention in the previous paper [4]. Our goal of this work is to present solid quantitative computations suggesting that this coherent $\mathcal{CP}$-odd axion field generates the disparity between nuggets and antinuggets. This asymmetry automatically leads to the relation (1) which we claim is a very generic consequence of the entire framework.

The readers who are not interested in any technical details may skip the next two sections (Secs. III and IV) and jump directly to the concluding Sec. V.

In Sec. III, we argue that the nuggets and antinuggets behave in a drastically different way as a result of interaction with this $\mathcal{CP}$-odd coherent cosmological axion field. Finally, in Sec. IV, we argue that the difference in the evolution of the nuggets and antinuggets is always of the order 1 effect, being insensitive to initial conditions and to the dynamical parameters of the system. As a result, the main claim of this proposal represented by Eq. (1) is a very robust consequence of the framework and is not a result of any fine-tuning adjustments.

II. BIG PICTURE AND THE CRUCIAL ELEMENTS OF THE PROPOSAL

In this section, we summarize the crucial elements of the proposal which describe the formation of the nuggets. These ingredients determine the basic properties of the nuggets, such as the size, local accretion of baryonic charge, abundance, stability, and global $\mathcal{CP}$-violating charge separation leading to the disparity between nuggets and antinuggets. Most of these basic elements of the proposal have been discussed previously in the original papers [1,4]. We include them in the present work to make it self-contained. One crucial ingredient of the proposal which was mentioned in Ref. [4] but has not been fully elaborated there is related to the $\mathcal{CP}$-violating processes leading to the asymmetry between nuggets and antinuggets. We highlight the basic idea on $\mathcal{CP}$ violation in Sec. II E,

while the detailed analysis of this ingredient of the proposal is carried out in "technical" Secs. III and IV.

A. $N_{\rm DW}=1$ domain walls

The first important element, the axion domain wall [36,37], determines the size of a nugget as originally suggested in Ref. [1]. The axion field θ is an angular variable and therefore supports various types of the topological domain walls (DW), including the so-called $N_{\rm DW}=1$ domain walls when θ interpolates between one and the same physical vacuum state with the same energy $\theta\to\theta+2\pi n$.

It is important to emphasize that, while the axion string formation happens during the Peccei-Quinn (PQ) phase transition, the domain-wall formation occurs at the QCD temperature at $T\sim 1$ GeV when the axion potential gets tilted. In other words, the formation of the DW-string network is the two-stage process, rather than a single event; see Ref. [37] for review. Furthermore, the DW energy density per unit volume is characterized by a typical QCD scale, rather than the PQ scale. Therefore, the closed DW surfaces, without attached strings, could be formed during the QCD transition, though the number density of such objects is suppressed with increasing the size of the objects [37,38]; see Sec. II C with a few more comments and estimates on this suppression.

One should also add that the numerical simulations [38] support this picture by observing the formation of the large DW at the QCD temperature and their decay due to the attached strings. The closed DW without attached strings have been also observed in numerical simulations [37,38], though the probability to find the closed walls is suppressed according to (4). Due to this suppression, the role of these closed DWs is normally ignored in the analysis of the DW decays to the DM axions. However, precisely these closed DW surfaces formed at the QCD scale play the key role in our proposal [1]; see additional comments at the end of this subsection.

One should remark here that it is normally assumed that for the topological defects to be formed, the PQ phase transition must occur after inflation. This argument is valid for a generic type of domain walls with $N_{DW}\neq 1$. The conventional argument is based on the fact that few physically *different vacua* with the same energy must be present inside of the same horizon for the domain walls to be formed. The $N_{DW}=1$ domain walls are unique and very special in the sense that θ interpolates between *one* and the *same* physical vacuum state. Such $N_{DW}=1$ domain walls can be formed even if the PQ phase transition occurred before inflation and a unique physical vacuum occupies the entire Universe [4].

In other words, while in our proposal the inflation is assumed to occur after the PQ phase transition and the axion field $\theta(t)$ is coherent in the entire visible Universe, nevertheless the $N_{DW}=1$ closed domain walls can still be formed. The nonzero θ would essentially lead to a global $\mathcal{CP}$-violating separation of baryonic charge as discussed in Sec. II E.

The axion domain walls normally start to form once the axion field gets tilted at temperature T_a. As the tilt becomes more pronounced (at the transition when the chiral condensate forms at T_c), the DW formation becomes much more efficient. We should expect, in general, that the $N_{\rm DW}=1$ domain walls form at any moment between T_a and T_c. The width of the domain wall depends on the mass of the axion, which would ultimately determine the size of the nugget being formed.

One next comment is as follows. It was realized many years after the original publication [36] that the axion domain walls generically demonstrate a sandwichlike substructure on the QCD scale $\Lambda_{\rm QCD}^{-1}\simeq$ fm. Such a substructure is supported by analysis [39] of QCD in the large N limit with the inclusion of the η' field. It is also supported by the analysis [40] of supersymmetric models where a similar θ vacuum structure occurs. The same structure also occurs in the color superconducting (CS) phase where the corresponding domain walls have been explicitly constructed [41].

The significance of the QCD substructure is that it is capable of squeezing the quarks to bring the system into the CS state, as originally suggested in Ref. [1]. The fact that the CS phase representing the lowest energy state might be realized in nature in the core of neutron stars has been known for quite sometime. A less known application of the CS phase is that the axion DW with the QCD substructure may replace the gravity and play the role of a squeezer to produce an absolutely stable quark nugget at $T=0$ as suggested in Ref. [1].

The time evolution of these nuggets at $T\neq 0$ is a much more involved problem than the study of the equilibrium configurations at $T=0$ carried out in Ref. [1]. The corresponding problem of the time evolution at $T\neq 0$ has been recently addressed in Ref. [4]. In particular, in that paper, it was shown that the nuggets assume the equilibrium at low temperature with the lowest possible state if the initial size of the nugget is sufficiently large. These results fully support the earlier studies of Ref. [1] devoted to the equilibrium configurations at $T=0$.

To conclude this subsection, the formation of the axion DW at the QCD transition is an extremely generic phenomenon which inevitably occurs as a result of $\theta\to\theta+2\pi n$ periodicity. These axion DWs typically have the QCD substructure as mentioned above. Furthermore, the formation of the closed surfaces at the QCD transition (which eventually may produce the quark nuggets) also represents a very generic feature of the system, which will be further elaborated in Sec. II C.

B. Spontaneous breaking of $\mathcal{C}$ symmetry on small scale of order $\xi(T)$

The second important element of the formation mechanism can be explained as follows. There is another

substructure with a similar QCD scale (in addition to the known substructures expressed in terms of the η' and gluon fields as explained in Sec. II A above) which carries the baryon charge. This additional substructure is a novel feature of the axion domain walls which has been explored only recently in Ref. [4]. As (anti)quarks being trapped in the core of the domain wall, the nuggets themselves slowly *accrete* the baryonic charge as a result of evolution. Exactly this new effect is eventually responsible for the local accretion of the baryonic charge by the nugget.

Indeed, in the background of the domain wall, the physics essentially depends on two variables, (t, z). One can show that in these circumstances, the total baryon charge B accumulated on a nugget is determined by the degeneracy factor in the vicinity of the domain wall [4],

$$B = N \cdot g \cdot \int \frac{d^2x_\perp d^2k_\perp}{(2\pi)^2} \frac{1}{\exp(\frac{\epsilon-\mu}{T}) + 1}. \tag{3}$$

In this formula, the induced baryon number N per degree of freedom may randomly assume any integer value, positive or negative; the coefficient g describes the degeneracy factor, e.g., $g \simeq N_c N_f$ in the CS phase, and μ is the chemical potential in the vicinity of the domain wall. Thus, the size distribution for quark and antiquark nuggets will be identically the same size if the external environment is $\mathcal{CP}$ even, which is the case when fundamental $\theta = 0$.

The crucial element here is that the domain walls will acquire the baryon or antibaryon charge as a generic feature of the system. This is because the domain-wall tension is mainly determined by the axion field while the QCD substructure leads to a small correction factor of order $\sim\Lambda_{\rm QCD}/f_a \ll 1$. Therefore, the presence of the QCD substructure with nonvanishing $N \neq 0$ increases the domain-wall tension only slightly. Consequently, this implies that the domain-wall closed bubbles carrying the baryon or antibaryon charge will be copiously produced during the transition as they are very *generic configurations of the system*. Furthermore, the baryonic charge cannot leave the system during the time evolution as it is strongly bound to the wall due to the topological reasons. The corresponding binding energy per quark is of order μ and increases with time as shown in Ref. [4]. One can interpret this phenomenon as a *local spontaneous breaking of $\mathcal{C}$ symmetry*, when on the scales of order the correlation length $\xi(T) \sim m_a^{-1}(T)$ the nuggets may acquire the positive or negative chemical potential μ with equal probability. This is because the sign of N in Eq. (3) may assume any positive or negative values with equal probabilities.

C. Kibble-Zurek mechanism

The Kibble-Zurek (KZ) mechanism gives a generic picture of formation of the topological defects during a phase transition. We refer to the original papers [42], a review [43], and the textbook [37] for a general overview. For our specific purposes of the DW formation, the KZ mechanism suggests that once the axion potential is sufficiently tilted, the $N_{\rm DW} = 1$ closed domain walls form at the QCD scale. Some time after T_a the system is dominated by a single, percolated, highly folded, and crumple domain-wall network of very complicated topology. In addition, there will be a finite portion of the closed walls (bubbles) with typical size of order the correlation length $\xi(T)$, which is defined as an average distance between folded domain walls at temperature T. Parametrically, the correlation length $\xi(T) \sim m_a^{-1}(T)$ is determined by the axion mass and obviously varies with time during the network evolution. Precisely these bubbles are capable of forming the nuggets and play the crucial role in our analysis. It is known that the probability n of finding closed walls with very large size $R \gg \xi$ is exponentially small, see Ref. [37] for a review,

$$n \sim \exp\left[-\frac{R^2}{\xi^2(T)}\right]. \tag{4}$$

The key point for our proposal is the mere existence of these finite closed bubbles made of the axion domain walls. Normally, it is assumed that these closed bubbles collapse as a result of the domain-wall pressure and do not play any significant role in the dynamics of the system because the total area of these bubbles is sufficiently small in comparison with the area of the dominant percolated domain-wall network. However, as we already mentioned in Sec. II A, some of these closed bubbles do not collapse due to the Fermi pressure acting inside of the bubbles. The equilibrium is achieved when the Fermi pressure from inside due to the degenerate quarks equals the pressure from outside due to the axion domain wall. This is precisely the condition of the stability analyzed in Ref. [1].

There are many papers devoted to analysis of the network made of the domain walls bounded by the strings. There are also many papers devoted to the problem (and its possible resolutions) on the domain-wall dominance of the Universe. We have nothing new to add to these subjects, and we refer to the original literature [38,44–47] and reviews [11,37] on this matter. Those axions (along with the axions produced by the conventional misalignment mechanism [44,48]) will contribute to the dark matter density today. The corresponding contribution to DM density is highly sensitive to the axion mass as $\Omega_{\rm dark} \sim m_a^{-7/6}$, and it is not part of our framework.

Instead, our proposal focuses on the dynamics of the closed bubbles (4), which are formed during the QCD transition. These closed bubbles are normally ignored in computations of the axion production. Precisely these closed bubbles will eventually become absolutely stable quark nuggets and may serve as the dark matter candidates according to the proposal [1,4].

The efficiency of the production of these bubbles has been estimated in Ref. [4], based on the assumption that this mechanism saturates the observed ratio $n_B/n_\gamma \sim 10^{-10}$. We shall not discuss this model-dependent estimate in the present work as the main goal of the present analysis is to demonstrate that $c(T) \sim 1$ in Eq. (8).

D. Color superconductivity

The existence of the CS phase in QCD is the crucial element for the stability of quark nuggets. In astrophysics, a CS is known to be the plausible phase in the neutron star interiors and in the violent events associated with the collapse of massive stars or collision of neutron stars; see the review papers [49,50] on the subject. The CS phase becomes energetically favorable when quarks are squeezed to a few times of nuclear density.

Analogous to the gravitational squeezing in a neutron star, the CS phase might be realized in quark nuggets due to the surface tension of the axion domain wall as advocated in Ref. [1]. The domain-wall bubbles after formation will undergo a large number of bounces with typical frequency $\omega \sim m_a$ until they settle down at the equilibrium configuration [4]. As the temperature cools down, the oscillations and squeezing will turn the bulk of quarks into an equilibrium position with the ground state being in the CS phase.

The corresponding time evolution of an oscillating bubble can be approximated[3] as follows,

$$R(t) = R_{\rm form} + (R_0 - R_{\rm form})e^{-t/\tau}\cos\omega t, \qquad (5)$$

where the initial radius of a bubble $R_0 \sim \xi(T)$ is assumed to be of order the correlation length $\xi(T)$. The final size $R_{\rm form}$ of a bubble represents the equilibrium configuration when formation is almost complete. In formula (5), parameter τ represents a typical damping time scale which is expressed in terms of the axion mass m_a and the QCD parameters such as viscosity. It turns out the numerical value of τ is of order the cosmological scale $\tau \sim 10^{-4}$s. This numerical value is fully consistent with our anticipation that the temperature of the Universe drops approximately by a factor of ∼3 or so during the formation period. During the same period of time, the chemical potential μ inside the nugget reaches a sufficiently large value when the CS phase sets in [4].

[3]One should emphasize that the simple analytical expression (5) is presented here for illustrative purposes to demonstrate the oscillating and damping features of the nugget's evolution. Numerically, it is only justified at the very end of the evolution when the amplitude of the oscillations is small, and a complicated effective potential can be expanded around its minimum as discussed in Ref. [4]; see also related discussions after Eq. (27). In other words, formula (5) properly describes the dynamics of the nugget only when the nugget's formation is almost complete. In our numerical studies given in Appendix D, we use the original potential without assuming that the oscillations are small.

E. Coherent $\mathcal{CP}$-odd axion field

The key element to be investigated in the present work is the $\mathcal{CP}$ asymmetric charge separation originating from the globally coherent axion field $\theta(t)$. In this subsection, we outline the basic ideas, while all technical details will be elaborated in Secs. III and IV.

It is well known that the axion dynamics at sufficiently large temperature $T > T_c$ is determined by the coherent state of axions at rest, see e.g., the review paper [11],

$$\theta(t) \sim \frac{C}{t^{3/4}}\cos\int^t dt'\omega_a(t'), \quad \omega_a^2(t) = m_a^2(t) + \frac{3}{16t^2}, \qquad (6)$$

where C is a constant and $t = \frac{1}{2H}$ is the cosmic time. This formula describes the dynamics of the axion field after the moment t_1 determined by the condition $m_a(t_1)t_1 = 1$ when the axion mass m_a effectively turns on at t_1. Precisely this moment is relevant for our studies as the domain walls start to form after t_1. For sufficiently large t when $m_a(t)t \gg 1$, the second term in the expression for $\omega_a^2(t)$ can be ignored, and the frequency of the oscillations $\omega_a(t)$ is determined by the axion mass at time t,

$$\dot\theta(t) \sim \omega_a(t) \simeq m_a(t). \qquad (7)$$

The key point in what follows is the observation that $\theta(t)$ is one and the same in the entire visible Universe. One should also emphasize that this assumption on the coherency of the axion field on very large scales is consistent with the formation of $N_{\rm DW} = 1$ domain walls as explained in Sec. II A.

Similar to the case of formation temperature $T_{\rm form}$ discussed in details in Ref. [4], precise dynamical computation of this $\mathcal{CP}$ asymmetry due to the coherent axion field $\theta(t)$ is a hard problem of strongly coupled QCD at $\theta \neq 0$ when even the phase diagram, schematically shown on Fig. 1, is not yet known. It depends on a number of specific properties of the nuggets, their evolution, their environment, modification of the hadron spectrum at $\theta \neq 0$, and corresponding cross sections as mentioned in Ref. [4]. All these factors equally contribute to the difference between the nuggets and antinuggets. One can effectively account for these coherent $\mathcal{CP}$-odd effects by introducing an unknown coefficient $c(T)$ of order 1 as follows [4]:

$$B_{\rm antinuggets} = c(T)\cdot B_{\rm nuggets}, \qquad \text{where } |c(T)| \sim 1. \qquad (8)$$

The main goal of the present work is to provide the quantitative numerical analysis supporting the basic assumption (8). We shall argue that $|c(T)| \sim 1$ is indeed very likely to be of order 1 as a result of the $\mathcal{CP}$-violating processes which took place coherently on the enormous scale of the entire visible Universe before the QCD transition. We shall argue below that this very generic outcome of this framework is not very sensitive to initial

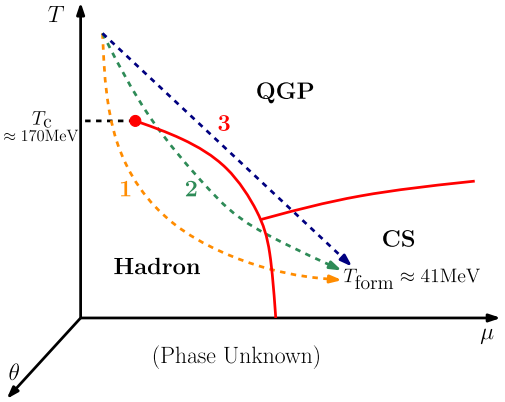

FIG. 1. The conjectured phase diagram. The plot is taken from Ref. [4]. Possible cooling paths are denoted as path 1, 2, or 3. The phase diagram is in fact much more complicated as the dependence on the third essential parameter; the θ is not shown as it is largely unknown. It is assumed that the final destination of the nuggets is the CS region with $T_{\rm form} \approx 41$ MeV, $\mu > \mu_c$, and $\theta \approx 0$.

conditions (such as the magnitude of θ_0 at the moment of formation), nor to a precise value of the axion mass $m_a(T)$ at $T > T_c$ when the domain-wall network only started to form. The fundamental ration (1) is the direct consequence of $|c(T)| \sim 1$. Therefore, the arguments supporting (8) are essentially equivalent to the basic claim of this framework (1).

What is the significance of Eq. (8)? The most important and unambiguous consequence of the Eq. (8) is that the baryon charge in the form of the visible matter can be also expressed in terms of the same coefficient $c(T) \sim 1$ as follows $B_{\rm visible} = -(B_{\rm antinuggets} + B_{\rm nuggets})$. Using Eq. (8), the expression for the visible matter $B_{\rm visible}$ can be rewritten as [4]

$$B_{\rm visible} \equiv (B_{\rm baryons} + B_{\rm antibaryons}) = -[1 + c(T)]B_{\rm nuggets} = -\left[1 + \frac{1}{c(T)}\right] B_{\rm antinuggets}. \tag{9}$$

This is a very important relation which we would like to represent in terms of the measured observables $\Omega_{\rm visible}$ and $\Omega_{\rm dark}$ at late times when the visible matter consists of the baryons only [4]:

$$\Omega_{\rm dark} \simeq \left(\frac{1 + |c(T)|}{|1 + c(T)|}\right) \cdot \Omega_{\rm visible} \quad \text{at } T \le T_{\rm form}. \tag{10}$$

An important comment here is that the relation (9) holds as long as the thermal equilibrium is maintained. Furthermore, the thermal equilibrium implies that each individual contribution $|B_{\rm baryons}| \sim |B_{\rm antibaryons}|$ entering (9) is many orders of magnitude greater than the baryon charge hidden in the form of the nuggets and antinuggets at earlier times when $T_c > T > T_{\rm form}$. However, the net baryon charge which is labeled as $B_{\rm visible}$ in Eq. (9) is the same order of magnitude as the net baryon charge hidden in the form of the nuggets and antinuggets.

For a specific value of $c(T_{\rm form}) \simeq -1.5$, the relations (9) and (10) assume the form

$$B_{\rm visible} \simeq \frac{1}{2} B_{\rm nuggets} \simeq -\frac{1}{3} B_{\rm antinuggets}, \qquad \Omega_{\rm dark} \simeq 5 \cdot \Omega_{\rm visible}. \tag{11}$$

These numerical values coincide with approximate relation (2) presented in the Introduction. The coefficient ∼5 in relation $\Omega_{\rm dark} \simeq 5 \cdot \Omega_{\rm visible}$ is obviously not universal, but relation (10) is universal and a very generic consequence of the entire framework, which was the main motivation for the proposal [1,2].

We shall argue in Secs. III and IV that $|c(T)| \sim 1$ is indeed of order 1. Furthermore, we shall argue that this feature of the system is universal and not very sensitive to the axion mass $m_a(T)$ nor to the initial value of θ_0 when the bubbles start to oscillate and slowly accrete the baryon charge. The only crucial factor in our arguments is that the axion field $\theta(t)$ can be represented by the coherent superposition of the axions at rest (6).

III. EVOLUTION OF THE (ANTI)NUGGETS IN THE BACKGROUND OF THE AXION FIELD

In this section, we study the profound consequences of the coherent axion phase on the nugget's formation. Essentially, the main goal of this section is to present analytical and numerical arguments suggesting that small $\mathcal{CP}$-violating effects will produce a large disparity (of order 1) between the nuggets and antinuggets.

We start with Sec. III A where we present some qualitative explanation of how a relatively small fundamental coupling between quarks/antiquarks and the coherent axion $\theta(t)$ field given by (6) may, nevertheless, produce a large asymmetry in properties between the nuggets and antinuggets. In Secs. III B and III C, we develop the technical tools to address these questions, while in Sec. III D, we present our estimates supporting the main claim of this work that $|c(T)| \sim 1$.

A. Qualitative analysis

Before we start our specific quantitative studies in this section, we want to formulate a few generic relations which characterize the system and which depend exclusively on symmetric features of the system, rather than on some specific dynamical model-dependent computations which follow.

First of all, let us remind the reader that if $\langle\theta\rangle = 0$, the baryon charge hidden in nuggets on average is equal to the baryon charge hidden in antinuggets, of course with sign

minus. Indeed, the studies of the antinuggets can be achieved by flipping the sign of the chemical potential $\mu \to -\mu$ in the analysis of Ref. [4]. One can restore the original form of the effective Lagrangian by flipping the sign for the axion θ field as discussed in Ref. [4]. These symmetry arguments imply that, as long as the pseudoscalar axion field θ fluctuates around zero $\langle\theta\rangle = 0$ as conventional pseudoscalar fields (such as π, η' mesons, for example), the theory remains invariant under $\mathcal{P}$ and $\mathcal{CP}$ symmetries, and on average, an equal number of nuggets and antinuggets carrying equal baryon (antibaryon) charges would form.

However, if $\langle\theta\rangle \neq 0$, there are many strong processes taking place inside and outside the nuggets (such as annihilation, evaporation, scattering, etc.), which are slightly different[4] for nuggets and antinuggets, as reviewed in Appendix A. Furthermore, the vacuum energy itself and the density of states in all these regions are also slightly different because the vacuum condensate (A4) assumes slightly different numerical values in all these regions as it depends on μ, T, and θ.

Precise computations of all these coherent $\mathcal{CP}$-violating QCD effects are hard to carry out explicitly as they require the solution of many body effects in an unfriendly environment with nonvanishing θ, μ, T when even the phase diagram is not yet known; see Fig. 1. However, the estimation of the effect is a very simple exercise as it must be proportional to $\theta(t)$ at the moment when the domain walls start to form. Numerically, this parameter $|\theta(t)/\theta_0| \sim 10^{-2}$–$10^{-3}$ could be quite small and naively may lead only to minor effects $\leq 10^{-2}$. However, the crucial point here is that, while this coupling is indeed small on the QCD scale, it is nevertheless effectively long ranged and long lasting, in contrast with conventional random QCD processes. As a result, these coherent $\mathcal{CP}$-violating effects will produce large effects of order 1 as explicit computations carried out below show.

The crucial element in making such an assessment is the observation that these small coherent changes occur in the entire volume of a nugget. In other words, the generation of the chemical potential, accumulation of the phase difference (which eventually leads to the accretion of the baryon charge), etc., are proportional to the volume of the nugget,

$$\Delta B \sim \theta(t) V, \qquad |\theta(t)/\theta_0| \sim 10^{-2}\text{–}10^{-3}, \tag{12}$$

where ΔB is the baryon charge difference in accumulation between the nuggets and antinuggets. This expression should be contrasted with effect due to the local spontaneous violation of the $\mathcal{C}$ symmetry (as discussed in Ref. [4] and reviewed in Sec. II B) which is proportional to the surface of a nugget, $B \sim S$; see Eq. (3).

While all individual events are proportional to small parameter $\theta \ll 1$, and therefore numerically small, this difference (between a typical size for nuggets vs antinuggets) eventually will be of order 1 as a result of long lasting evolution, as is shown in the next subsections. This strong effect of order 1 has been phenomenologically accounted for by parameter $c(T)$ in formula (8), which automatically leads to the main consequence of this framework expressed by relation (1).

B. Basic equations

We start with a brief overview of the work [4], where it was assumed that the $\mathcal{CP}$ symmetry is globally conserved, i.e., $\langle\theta(t)\rangle = 0$ when averaged over the entire Universe. In that paper, the effective interaction of the axion domain wall with Fermi fields was approximated as follows,

$$\mathcal{L}_4 = \bar{\Psi}(i\partial\!\!\!/ - m e^{i[\theta(x)-\phi(x)]\gamma_5} - \mu\gamma_0)\Psi, \tag{13}$$

where parameter m should not be interpreted as the quark's mass. Rather, it is much more appropriate to interpret parameter m as the expectation value of the $\langle \det \bar{\psi}^f_L \psi^f_R \rangle$ from Eq. (A4) which has a typical QCD scale and which will always be generated even in the deconfined regime at $T > T_c$. The Fermi field Ψ should be interpreted as the low-energy (soft) component of the original quark fields, while a high-energy component has been integrated out to generate parameter m entering (13). Equation (13) is the standard form for the interaction between the pseudoscalar fields [axion $\theta(x)$ and η' field parametrized by $\phi(x)$] and the fermions (quarks and antiquarks) which respect all relevant symmetries in the presence of nonzero chemical potential μ.

Another key element from Ref. [4] which is relevant for our present studies is the effective Lagrangian describing the dynamics of an oscillating domain-wall bubble,

$$L = \frac{4\pi\sigma R^2(t)}{2}\dot{R}^2(t) - 4\pi\sigma R^2(t) + \frac{4\pi R^3(t)}{3}\Delta P(\mu) + [\text{other terms}]. \tag{14}$$

Equation (14) describes the time evolution of the closed spherically symmetric domain-wall bubble of radius $R(t)$. The pressure term $\Delta P = P^{(\text{Fermi})} + P^{(\text{Bag})} - P^{(\text{out})}$ in Eq. (14) can be parametrized as [4]

$$\Delta P = \frac{g^{\text{in}} T^4}{6\pi^2} I_4(b) - E_B \theta(b - b_1)\left(1 - \frac{b_1^2}{b^2}\right) - \frac{\pi^2 g^{\text{out}} T^4}{90},$$

[4]In particular, a slight difference of the ground states characterized by the condensate (A4) leads to the different properties of the quasiparticles and scattering amplitudes inside and outside the nuggets due to μ dependence of the θ-dependent condensate (A4). The same effects also contribute to some disparity in transmission/reflection coefficients, minor differences in viscosity, annihilation and evaporation rates, etc.

where $g^{\rm in} \simeq 2N_cN_f$ and $g^{\rm out} \simeq (\frac{7}{8}4N_cN_f + 2(N_c^2-1))$ are degeneracy factors for inside and outside of the bubble, respectively; $b = |\mu|/T$ is the dimensionless parameter to be used frequently in what follows; $I_4(b)$ is a specific type of Fermi integrals (see Appendix E); and finally $E_B \sim (150\ {\rm MeV})^4$ is the famous "bag constant" from the MIT bag model, which turns on in the hadronic phase at small $\mu < \mu_1$, while it vanishes in the CS phase at large $\mu > \mu_1$.

The evolution of the bubble is governed by the following differential equations [4],

$$\frac{d}{dt}B_{\rm wall} = 0, \qquad B_{\rm wall} = \frac{g^{\rm in}ST^2}{2\pi}I_2(b) \tag{15a}$$

$$\sigma\ddot{R} = -\frac{2\sigma}{R} - \frac{\sigma\dot{R}^2}{R} + \Delta P(b) - 4\eta\frac{\dot{R}}{R}, \tag{15b}$$

where $\sigma \simeq 9f_a^2m_a$ is the domain-wall tension, while $\eta \simeq m_\pi^3$ is the QCD viscosity. The baryonic charge for nuggets can be expressed in terms of the Fermi integral $I_2(b)$ given in Appendix E. Equation (15a) describes an implicit dependence of the chemical potential on the size of the nugget, $\mu(R)$. It should be substituted to Eq. (15b) to arrive at the differential equation which describes the time evolution of the nugget $R(t)$. The corresponding analysis has been performed in Ref. [4] with the basic result that the solution can be well approximated by slow damping oscillations with typical frequency m_a around $R_{\rm form}$ as presented by Eq. (5).

As we already mentioned, in the preceding studies [4] on the bubble evolution, we had assumed that the $\mathcal{CP}$ symmetry is conserved as no interaction with the coherent axion field $\theta(t)$ was included in the consideration. Now, we wish to include the coherent axion field $\theta(t)$, given by Eq. (6) in the equations. The most important change which occurs as a result of the interaction of the Fermi fields with the background axion field is the accumulation of the phase (A2) as a result of the coupling Ψ field with axion field $\theta(t)$, which can be interpreted as the coherent Berry's phase, as explained in Appendix A.

To proceed with the computations, one could follow the procedure developed in Ref. [4], rewrite the Fermi fields in 2D notations (accounting for the domain-wall background), and represent the extra term to the effective Lagrangian due to the coupling with external axion field as follows,

$$\Delta\mathcal{S} = -\frac{1}{\pi}\int dz\mu(z)\partial_z\theta(t),$$
$$A \equiv -\frac{\delta\Delta\mathcal{S}}{\delta\mu} = \frac{1}{\pi}\int_{R_{\rm in}}^{R_{\rm out}} dz\cdot\left(\frac{\partial\theta}{\partial t}\right)\frac{1}{\dot{R}}, \tag{16}$$

where the end points of the integral $z = (R_{\rm in}, R_{\rm out})$ should be interpreted as the typical distances describing the regions inside and outside the bubble of a typical size $z \simeq R$.

A few comments are in order. First, one can explicitly see from Eq. (16) that the effect is different for nuggets and antinuggets as the sign of μ is opposite in these cases, while the background field $\theta(t)$ remains the same in the entire visible Universe. Secondly, parameter A can be interpreted as an additional baryon charge (per degree of freedom) accumulated by a nugget during a single nugget's cycle. This coefficient can be approximated as follows,

$$A \simeq \frac{\Delta\theta}{\pi}, \tag{17}$$

where $\Delta\theta$ can be interpreted as the variation of the axion field during a single-nugget's cycle. One should emphasize that the correction (17) is not the only source leading to the disparity between nuggets and antinuggets. In fact, many other $\mathcal{CP}$-violating processes may also contribute to the differences in accumulating baryon charges for nuggets and antinuggets. We expect that all these effects mentioned in footnote 4 are equally important as they must be proportional to the $\mathcal{CP}$-violating parameter $\theta(t)$. Therefore, the corresponding effects may be effectively accounted for by a modification of the numerical coefficient A entering (17). As we argue below, the outcome of the calculations is not very sensitive to a specific value of coefficient A. Therefore, neglecting a large number of different $\mathcal{CP}$-violating processes mentioned in footnote 4 (which can be accounted for by modifying the numerical coefficient A) does not affect the main result of our analysis.

Our next remark is the observation that the phase (6) and corresponding extra energy (16) are accumulated coherently by a large portion of quarks inside of a nugget of volume V, while the corresponding correction to the vacuum energy obviously vanishes outside the nuggets where $\mu \simeq 0$. To compute the correction to the baryon charge of a nugget due the coupling to the axion θ field, one should multiply (17) to the degeneracy factor, i.e.,

$$B_\theta^{(\pm)} = \pm g^{\rm in}AV\int\frac{d^3k}{(2\pi)^3}\frac{1}{\exp(\frac{k}{T}-b)+1}$$
$$= \pm\left(\frac{g^{\rm in}ST^2}{2\pi}I_2^{(\pm)}(b)\right)\cdot\left(\frac{ART}{3\pi}\frac{I_3^{(\pm)}(b)}{I_2^{(\pm)}(b)}\right), \tag{18}$$

where we assume that the chemical equilibration is sufficiently fast such that one can use one and the same μ within the entire volume of the nugget. Furthermore, in writing down Eq. (18), we assumed that the majority of quarks in volume V move coherently during the bubble oscillations. In fact, the coherence might not be so perfect, and only some portion of the quarks inside the nuggets might move coherently as a macroscopical system. It is very hard to estimate the corresponding suppression factor within our framework formulated in terms of a single macroscopical variable $R(t)$. The corresponding suppression factor may

be effectively accounted for by some modification of the numerical coefficient A entering (18). As we already previously mentioned, our results are not very sensitive to an absolute value of the numerical value of A as long as it is not exceedingly small. Therefore, we assume that all correction factors mentioned previously in footnote 4 and the suppression factor due to not perfect coherent motion are implicitly included in coefficient A in the analysis which follows.

Our next remark goes as follows. In Eq. (18), we presented the expression for $B_\theta^{(\pm)}$ as a combination of two factors. The first factor is precisely the expression for the baryon charge $B_{\rm wall}$ from Eq. (15a) generated spontaneously as described in Ref. [4]. The second factor represents the correction to the accumulated baryon charge due to the coupling of the $\mathcal{CP}$-odd axion field with quarks inside the nugget. It is important to emphasize that it is numerically suppressed due to the small $\mathcal{CP}$-violating phase (6) parametrized by small numerical coefficient A. However, it is strongly enhanced by a large numerical factor proportional to the size of the system. In contrast to the baryon accumulation in Eq. (15a) which is proportional to the surface, the $B_\theta^{(\pm)}$ contribution is proportional to the volume of the system (18), in agreement with qualitative arguments (12) of the previous section.

Our next comment is as follows. Naively, one could think that the accumulation of the baryon charge by a nugget due to the coherent interaction with the axion field θ will be very fast since it is proportional to the volume V of the nugget according to (18). However, the accumulation is in fact quite slow. The point is that the axion θ field oscillates with time, $\sim\cos(m_a t)$, and the accumulated baryon charge is almost washed out during a complete cycle of the axion $\theta(t)$ field. Nevertheless, the cancellation is not quite complete because the axion field slowly reduces its amplitude. The main reason for this amplitude's decay is the emission of real physical axions (due to the misalignment mechanism) which is the source of some nonequilibrium dynamics. Precisely this slow decrease of the axion amplitude leads to a nonvanishing $\Delta\theta$ entering (17) and eventually generates the disparity between nuggets and antinuggets.

To recapitulate, a tiny portion of the accumulated baryon charge remains in the nuggets after every single complete cycle such that the disparity between nuggets and antinuggets will be accumulated but at very slow pace as a result of very large number of oscillations. Based on this fact, we can therefore assume A as an adiabatic "constant" for each given cycle in the analysis in the following Secs. III C and III D.

Our final remark regarding Eq. (18) is as follows. This formula was derived by considering the coherently moving quarks of the nuggets in the background of the axion field (6). This approximation is only justified as long as the effect due to the background field is sufficiently small. Formally, the effect (18) due to the axion field must be much smaller than the initial accumulation of the baryon charge (15a) due to the spontaneous local symmetry breaking when the original chemical potential μ is generated. Such a condition must be imposed on our system to avoid any complications related to accounting for the feedback (backreaction) of the coherent Fermi field on the background field. We satisfy this condition by requiring that the expression in the second bracket in (18) is (marginally) smaller than unity, i.e.,

$$\frac{B_\theta^{(\pm)}}{B_{\rm wall}}\sim\left(\frac{ART}{3\pi}\frac{I_3^{(\pm)}(b)}{I_2^{(\pm)}(b)}\right)\lesssim 1. \tag{19}$$

This condition can be also understood as the requirement that the accreted baryon charge $B_\theta^{(\pm)}$ due to the background field does not change the original boundary conditions imposed on the quark's fields in the domain-wall background. Precisely these boundary conditions determine the sign of the $B_{\rm wall}$ as a result of the local spontaneous symmetry breaking effect as discussed in Ref. [4].

Furthermore, precisely these boundary conditions generate the initial chemical potential of a nugget which enters (16). The requirement (19) states that the influence of $B_\theta^{(\pm)}$ on the initial axion domain-wall background should be sufficiently small. Although condition (19) is exact, it is not technically useful to implement in the following analysis because it contains complicated functions of R and μ. To get rid of such cumbersome dependence, we use the fact $I_3(b)/I_2(b)$ can be approximated for small μ with sufficiently high accuracy as $I_3(b)/I_2(b)\simeq 3/2$ at $b=|\mu|/T\ll 1$; see Appendix E. With this approximation, we obtain a much more useful, practical, and transparent condition,

$$a(t)\equiv\frac{AR_0T}{2\pi}\simeq\left|\frac{B_\theta^{(\pm)}}{B_{\rm wall}}\right|,\qquad |a(t)|\lesssim 1. \tag{20}$$

Note that we define this simplified condition in terms of a single parameter $a(t)$. By monitoring the value of $a(t)\lesssim 1$, we can precisely determine whether our analysis is valid and justified or if it is about to break down. In what follows, we will express the formula in terms of $a(t)$ up to the linear order since we are only interested in the region of sufficiently small $a\lesssim 1$ where our analysis is marginally justified. It is quite obvious that $a(t)$ can be treated as an adiabatic parameter slowly changing with time as the typical time scale for variation $a(t)$ is determined by changing of the axion field during a single cycle (17).

After these comments, we can now follow the procedure developed in Ref. [4] to account for the $\mathcal{CP}$-violating effects by replacing Eq. (15a) by its generalized version in the form

$$\frac{d}{dt}(B_{\rm wall}+B_\theta^{(\pm)})=0. \tag{21}$$

Similarly to Ref. [4], we treat Eq. (21) as an implicit relation between $\mu(t)$ and $R(t)$ which should be substituted into Eq. (15b) to arrive at a single differential equation which governs the dynamics of $R(t)$ as a function of time t,

$$\sigma\ddot{R}(t) = -\frac{2\sigma}{R} - \frac{\sigma\dot{R}^2}{R} + \Delta P^{\pm}[R] - 4\eta\frac{\dot{R}}{R}, \qquad (22)$$

where the pressure term is now a function of bubble radius $R(t)$, rather than μ. It can be approximated as follows,

$$\Delta P^{(\pm)}[R] \simeq \frac{g^{\rm in}T^4}{6\pi^2}[2\pi f^{(\pm)}(R) + (f^{(\pm)}(R))^2] - \frac{\pi^2 g^{\rm out}}{90}T^4 - E_B\theta(b-b_1)\left(1-\frac{b_1^2}{b^2}\right), \qquad (23)$$

where functions $f^{(\pm)}(R)$ entering (23) have been computed in Appendix C and can be approximated as follows:

$$f^{(\pm)}(R) \simeq \frac{\pi^2}{12}\frac{T_0^2R_0^2}{T^2R^2}\left[1 \mp a\left(\frac{4}{9}\frac{T_0}{T}\sqrt{\frac{\pi^2}{12}} + \frac{R}{R_0}\right)\right]. \qquad (24)$$

The new element in comparison with our previous studies [4] is that the pressure $\Delta P^{(\pm)}[R]$ is now different for nuggets and antinuggets because the functions $f^{(\pm)}(R)$ which determine their dynamics are quite distinct. The corresponding difference is determined by the coefficient (20) which is explicitly proportional to the $\mathcal{CP}$-odd parameter A as defined by Eqs. (16) and (17). Precisely this difference, as we discuss below, determines the imbalance in the evolution of the nuggets and antinuggets.

In what follows, we keep the temperature T to be constant, and furthermore we shall assume $T_0/T \simeq 1$ to simplify our numerical analysis. The justification for the first assumption (the temperature T is kept constant) is that all relevant processes (including the nugget's oscillations) have the time scales which are much shorter than a typical cosmological time scale when temperature T and the axion mass $m_a(T)$ slowly vary.

Indeed, as the temperature scales with cosmic time as $T \sim t^{-1/2}$, the corresponding variations of the temperature during a single axion oscillation, determined by time $\Delta t \sim m_a^{-1}$, are very tiny, $\Delta T/T \sim \Delta t/t \sim (m_a t)^{-1}$. Numerically, it represents extremely small correction $\Delta T/T \sim 10^{-5}$ for $m_a \sim 10^{-6}$ eV as the cosmic time t corresponding to the temperature T_0 is of order $t \sim 10^{-4}$s. It is known that the axion mass $m_a(T)$ experiences very sharp changes with the temperature $m_a(T) \sim T^{-n}$ with exponent $n \sim 8$; see Refs. [30–33]. Nevertheless, the axion mass does not vary much during a single axion oscillation. Indeed, during time $\Delta t \sim m_a^{-1}$, the axion mass receives a very tiny correction, $\Delta m_a/m_a \sim n(\Delta T/T) \sim n(m_a t)^{-1} \ll 1$.

Furthermore, one can argue that the nuggets make a very large number of oscillations during a few cycles of the axion field θ when the axion mass $m_a(T)$ and the temperature T experience very insignificant relative corrections. This justifies our assumption that $m_a(T)$ and T can be kept constant in our studies of the nugget's dynamics. We refer to Appendix D with corresponding estimates and details.

One can rephrase these arguments in slightly different way as follows. A slow change of the temperature T and the axion mass $m_a(T)$ is accompanied by slow variation of the axion amplitude $\theta(t)$. Precisely this θ variation eventually leads to the slow accumulation of the disparity between nuggets and antinuggets as argued below. The effects of variation of the dynamical equations such as (22) due to tiny changes of the temperature and the axion mass $\Delta T, \Delta m_a$ do not affect our analysis because the main source of the disparity is explicitly proportional to the chemical potential μ according to Eq. (16), while the small changes of temperature and the axion mass $\Delta T, \Delta m_a$ during the evolution contribute equally to both types of species and play the subleading role.

Another assumption ($T_0/T \simeq 1$) represents a pure technical simplification in our analysis to demonstrate that the disparity in evolution for different species is of the order 1 effect. In fact, one can argue that this imbalance (between the nuggets and antinuggets) becomes even more pronounced if one accounts for the decrease of temperature with time.

In principle, Eq. (22) can be solved numerically (without a large number of simplifications and assumptions mentioned above), which would determine the dependence of $R(t)$ and $\mu(t)$ on time. The corresponding results of these numerical studies are presented in Appendix D. These numerical results are fully consistent with our analytical (simplified) treatment of the problem, which is the subject of Secs. III C and III D.

C. Time evolution

First, we find the equilibrium condition when the "potential" energy in Eq. (22) assumes its minimal value, similar to the procedure carried out in Ref. [4]. The corresponding minimum condition is determined by the equation

$$\frac{2\sigma}{R_{\rm form}} = \Delta P^{(\pm)}[R_{\rm form}], \qquad (25)$$

where $\Delta P^{(\pm)}$ is defined by Eq. (23). The difference with the previously studied case [4] is that $\Delta P^{(\pm)}$ is now different for nuggets and antinuggets. Therefore, the equilibrium solution $R^{(\pm)}_{\rm form}$ will be also different for two different species. This is the key point of the present studies. Another distinct feature is that $R^{(\pm)}_{\rm form}$ slowly varies with time because the axion background adiabatically changes with time. The corresponding variation explicitly enters Eq. (21) and implicitly enters Eq. (22).

For the next step, we want to see how these different equilibrium solutions are approached when time evolves. We follow the conventional technique and expand (22) around the equilibrium values $R^{(\pm)}_{\rm form}$ to arrive at an equation for a simple damping oscillator,

$$\frac{d^2\delta R^{(\pm)}}{dt^2}+\frac{2}{\tau^{(\pm)}}\frac{d\delta R^{(\pm)}}{dt}+(\omega^{(\pm)})^2\delta R^{(\pm)}=0, \quad (26)$$

where $\delta R^{(\pm)}\equiv[R(t)-R^{(\pm)}_{\rm form}]$ describes the deviation from the equilibrium position, while new parameters $\tau^{(\pm)}$ and $\omega^{(\pm)}$ describe the effective damping coefficient and frequency of the oscillations. Both new coefficients are expressed in terms of the original parameters entering (22) and are given by

$$\tau^{(\pm)}=\frac{\sigma}{2\eta}R^{(\pm)}_{\rm form} \quad (27a)$$

$$(\omega^{(\pm)})^2=-\frac{1}{\sigma}\frac{d\Delta P^{(\pm)}(R)}{dR}\bigg|_{R^{(\pm)}_{\rm form}}-\frac{2}{[R^{(\pm)}_{\rm form}]^2}. \quad (27b)$$

The expansion (26) is justified, of course, only for small oscillations about the minimum determined by Eq. (25), while the oscillations determined by original equation (22) are obviously not small. However, our simple analytical treatment (26) is quite instructive and gives a good qualitative understanding of the system. The difference with previously studied case [4] is, of course, the emergence of two different solutions for two different species characterized by parameters (27) which also slowly vary with time. Our numerical studies presented in Appendix D fully support the qualitative picture presented in this subsection.

The most important conclusion of these studies is that nuggets and antinuggets oscillate in very much the same way as we observed in our previous studies and well approximated by Eq. (5). However, their evolution proceeds in a somewhat different manner now as a result of $\mathcal{CP}$-violating terms as discussed above.

To analyze this difference in a quantitative way, we introduce parameter $\Delta R(t)\equiv|R^+(t)-R^-(t)|$ which measures this difference between nuggets' and antinuggets' sizes, assuming that the same initial conditions are imposed, i.e., $R^{\pm}_0=R_0\sim m_a^{-1}$. The parameter $\Delta R(t)$ is the most important quantitative characteristic for our present studies as it shows how the sizes of nuggets and antinuggets evolve with time. We shall demonstrate that $\Delta R/R$ becomes of order 1 when the condition (20) is still marginally satisfied. Our simplified computations (by neglecting the backreaction which modifies the background) obviously break down when the ratio (20) approaches 1. However, once a sufficiently large effect is generated, we do not expect that it can be completely washed out by further evolution. Rather, it is expected that, once a large effect is generated, it remains to be a sufficiently large effect of order 1, though a precise numerical coefficient might be different from our qualitative analysis. In fact, the precise magnitude of $\Delta R/R$ is very hard to compute as there are many other effects mentioned in footnote 4 which influence the time evolution and equally contribute to $\Delta R/R$.

Therefore, the key result of our analysis is that $\Delta R(t)$ fluctuates with time but always approaches a nonvanishing magnitude of order 1 during the long cosmological evolution. The fluctuations for $R^{\pm}(t)$ are well approximated by Eq. (5), where key parameters (27) now are different for different species. Numerical results presented in Fig. 2 support this qualitative analysis presented above.

D. Disparity in sizes for nuggets and antinuggets

While numerical results presented in Fig. 2 explicitly show that the difference between typical sizes of nuggets and antinuggets becomes of the order 1 effect during the time evolution, we would like to understand this important feature of the system using analytical, rather than numerical, arguments. This subsection is devoted precisely to such an analysis.

In what follows, we would like to estimate $\Delta R(t)\equiv|R^+(t)-R^-(t)|$ at $t\to\infty$ when the system approaches its equilibrium; i.e., we are interested in the difference $\Delta R_{\rm form}\equiv|R^+_{\rm form}-R^-_{\rm form}|$ between nuggets and antinuggets. The equilibrium values for each species can be approximated as

$$\frac{2\sigma}{R_{\rm form}}\simeq\frac{g^{\rm in}T^4}{6\pi^2}[f^{(\pm)}(R_{\rm form})]^2, \quad (28)$$

where we simplified the original equations (23) and (25) by keeping the numerically dominant terms in the region where a typical radius of a nugget is considerably dropped from its initial value, i.e., $R_{\rm form}\lesssim 0.5R_0$; see Appendix D for details. For further simplifications and for illustrative purposes, we keep only the leading terms $\sim a$, similar to Eq. (24). Precisely these terms eventually lead to the disparity between nuggets and antinuggets, as we already discussed. With these simplifications, the formation radius for nuggets and antinuggets can be approximated as follows,

$$R^{\pm}_{\rm form}\simeq\langle R_{\rm form}\rangle\cdot\left[1\mp\frac{2a_c}{3}\left(\frac{\langle R_{\rm form}\rangle}{R_0}+\frac{2\pi}{9\sqrt{3}}\right)\right], \quad (29)$$

where $\langle R_{\rm form}\rangle$ is defined as the average size of different species,

$$\langle R_{\rm form}\rangle\equiv\frac{1}{2}|R^+_{\rm form}+R^-_{\rm form}|\simeq R_0\left[\frac{\pi^2 g^{\rm in}T^4}{12^3}\frac{R_0}{\sigma(T)}\right]^{1/3}, \quad (30)$$

while a_c is defined as the critical value at so-called decoherence time, $t_{\rm dec}$, when the axion field is losing

its coherence[5] on the scale of the Universe, such that the disparity between nuggets and antinuggets does not further evolve after $t_{\rm dec}$,

$$a_c \equiv a(t \to t_{\rm dec}), \qquad a_c < 1. \tag{31}$$

In Eq. (31), we also assumed that $a_c < 1$ is sufficiently small when the condition (20) is marginally satisfied.

A few comments regarding (29) and (30) are in order. First of all, as we already mentioned, we kept the temperature T to be constant in our computations. We can now treat T in (30) as an adiabatic parameter which slowly decreases with time as the temperature slowly approaches the QCD transition temperature T_c from above. During this evolution, the domain-wall tension $\sigma(T)$ approaches its final value $\sigma \to 9 f_a^2 m_a$ at the QCD transition point $T = T_c$ where the chiral condensate forms. This slow change of the formation radius $\langle R_{\rm form}\rangle$ is perfectly consistent with the numerical results presented in Fig. 2.

Second, using Eq. (29) and our estimate (30) for $\langle R_{\rm form}\rangle \simeq 0.6 R_0$, one can approximate the disparity in sizes $\Delta R_{\rm form}$ between two different species as follows:

$$\frac{\Delta R_{\rm form}}{\langle R_{\rm form}\rangle} \simeq \frac{4}{3}\cdot a_c. \tag{32}$$

This estimation suggests that the difference in baryon charges between the nuggets and antinuggets can be approximated as follows:

$$\frac{\Delta B}{\langle B\rangle} \simeq \left(\frac{\Delta R}{\langle R_{\rm form}\rangle}\right)^3 \simeq 3\frac{\Delta R}{\langle R_{\rm form}\rangle} \simeq 4 a_c. \tag{33}$$

In other words, even for relatively small $a_c \simeq (0.1 - 0.2)$ where our background approximation remains marginally valid according to condition (20), the disparity in baryon charges (33) between nuggets and antinuggets could be quite large and can easily satisfy the basic assumption (8) with $|c(T)| \sim 1$.

Our last comment is to elaborate on the physical meaning of parameter $a(t)$ which is defined by (20). This parameter enters (33) and plays an important role in our discussions and estimates which follow. The phenomenological parameter $a(t)$ has been introduced into our analysis to describe a very small variation (17) of the axion field after each single cycle during the nuggets' evolution. If the axion field were perfectly periodic with the original amplitude θ_0 being kept constant, then our parameter $a(t)$ would be identically zero as every consequent cycle of the axion field would wash out the asymmetry it produces during a previous cycle, as we already mentioned at the end of Sec. III B. However, the axion coherent field decays as a result of the production of the real propagating axions (as well as a result of many other processes mentioned in footnote 4). We parametrize these changes of the system by a function $a(t)$ assuming that initially $a(t = 0) = 0$ vanishes but slowly increases its value during the nugget's evolution. It reaches the maximum value a_c when the largest possible disparity between nuggets and antinuggets is achieved[6] as determined by Eq. (33). The disparity (33) cannot be washed out after $t_{\rm dec}$, as we discuss in the Sec. IV, because the axion field has lost its coherence on the scale of the Universe and cannot wash out the previously generated imbalance (33).

We conclude this section with the following remark. The main goal of this section was to demonstrate that even relatively small $\mathcal{CP}$-violating coupling (16), (17) of the coherent axion field with quarks (antiquarks) inside the nuggets (antinuggets) generically produces a large effect of order 1 as a result of a coherent long lasting influence of the axion field on the dynamics of the nuggets. We presented some semianalytical estimates expressed by Eq. (33) supporting this claim. The numerical results, obtained without a large number of simplifications and presented in Appendix D (see specifically Fig. 2) also reinforce the analytical analysis of this subsection.

The significance of the result (33) is that the disparity between nuggets and antinuggets unambiguously implies that our main assumption formulated as Eq. (8) is strongly supported by the computations of this section. Needless to say, Eq. (8) is essentially equivalent to our generic fundamental consequence (1) of this framework, suggesting that the visible and dark matter densities are of the same order of magnitude $\Omega_{\rm dark} \approx \Omega_{\rm visible}$ irrespectively of the parameters of the system.

IV. ROBUSTNESS OF THE IMBALANCE BETWEEN NUGGETS AND ANTINUGGETS

In this section, we would like to argue that the results of Sec. III are very robust in the sense that they are not very sensitive to the fundamental parameters of the system such as the axion mass m_a or initial misalignment angle θ_0. In particular, we shall argue in Sec. IV A that the results of the previous section are also insensitive to a large number of technical simplifications we have made in the previous section. Furthermore, we also present some arguments in Sec. IV B that the imbalance (33) survives the subsequent

[5]The decoherence time, $t_{\rm dec}$, is determined by a number of different processes, including the time scale for the axion field to decay into the randomly distributed DM axions; see footnote 13 in Ref. [4] for comments on this matter.

[6]In our numerical studies, we also assume that $a(t)$ never becomes too big, which would violate our approximations and would change the boundary condition imposed by the sign of the chemical potential μ as expressed by Eq. (19). We shall make a few technical comments in Sec. IV B on how to proceed with computations if parameter $a(t)$ becomes numerically large and our treatment of $a(t)$ as a small correction obviously breaks down.

evolution of the system at $t > t_{\rm dec}$ after the axion field loses its coherence.

A. Insensitivity to the axion mass m_a and initial misalignment angle θ_0

First of all, we want to argue that the disparity between nuggets and antinuggets expressed by Eq. (33) is not very sensitive to the axion mass m_a which itself varies with the temperature in the range $T_a \leq T \leq T_c$ and approaches its final value at the QCD transition at T_c, as explained in Sec. II. As a result of this "insensitivity" of Eq. (33) to m_a, the main consequence of the entire framework expressed as Eqs. (1) and (8) is also insensitive to the axion mass.

The main reason for this claim is that we are interested in the relative ratio (33) between nuggets and antinuggets rather than in the absolute value $\langle R_{\rm form}\rangle$ of a nugget, which is obviously sensitive to the axion mass as it scales as $\langle R_{\rm form}\rangle \sim m_a^{-1}$ according to (30). The ratio (33), on other hand, is not very sensitive to the absolute value of the axion mass. This feature is manifestly seen in Fig. 2 where two plots for $m_a = 10^{-4}$ eV and $m_a = 10^{-6}$ eV are almost identically the same.

To summarize the argument regarding the axion mass, the size of a nugget and its total baryon charge are highly sensitive to axion mass m_a. However, their relative ratio (33), which is equivalent to the basic relation (8), is always of order 1 and largely m_a independent. This basic feature eventually leads to a fundamental prediction of this framework, $\Omega_{\rm dark} \approx \Omega_{\rm visible}$, which is insensitive to the axion mass m_a, in contrast with conventional mechanisms of the axion production when $\Omega_{\rm dark} \sim m_a^{-7/6}$; see recent reviews [9–16].

Consequentially, we want to argue that the disparity between nuggets and antinuggets expressed by Eq. (33) is not very sensitive to the initial conditions of the misalignment angle θ_0. This is because the disparity (33) is determined by parameter $A \simeq \Delta\theta/\pi$ from Eq. (17), which has a meaning of the accumulated changes during a single cycle. The total accumulation of the changes during a large number of cycles is determined by the relation (20) which slowly approaches some constant value a_c irrespectively of what the original misalignment angle θ_0 at the initial time was.

In other words, if the initial θ_0 was quite small, then it might take a longer period of time before the coefficient $a(t)$ assumes its final value a_c. If the initial θ_0 was sufficiently large, it might take a slightly shorter period of time to get to the point when $a(t)$ approaches its finite value (31). However, in all cases, the coefficient $a(t)$ approaches the constant value (31) of order 1 due to the parametrically enhanced factor $\sim R_0 T$ in Eq. (20) such that even a very tiny initial magnitude of $a(t)$ generates an order 1 effect due to the long lasting coherent axion field as explained in the text after Eq. (33). This behavior should be contrasted with conventional mechanisms of the axion production when $\Omega_{\rm dark} \sim \theta_0^2$ is highly sensitive to initial misalignment angle θ_0; see recent reviews [9–16].

The same argument also applies to the initial T_0. To be more specific, the final result for the disparity is not very sensitive to the initial temperature T_0 as the relative imbalance (33) is essentially determined by the final value a_c rather than by some dynamical features of the system.[7]

Another important dimensional parameter of the system is viscosity η which, in particular, enters Eq. (27) and determines the frequency of oscillations $\omega^{(\pm)}$ and effective damping coefficient $\tau^{(\pm)}$ during the evolution. The sizes of the nuggets $R^{\pm}(t)$ are obviously very sensitive to these parameters $\omega^{(\pm)}$ and $\tau^{(\pm)}$ and, therefore, to viscosity η. However, as in our previous discussions, the disparity (33), which is a dimensionless parameter measuring the relative sizes on different species, is not sensitive to this parameter when computed at the very end of the evolution. In other words, it might take a longer (or shorter) period of time for different values of η to get to the final destination determined by Eq. (33). However, the numerical value of the disparity (33) always remains the same and determined by parameter a_c when the axion (initially coherent) field has lost its conference. To demonstrate this feature, we present the behavior of the system for two different values of the viscosity η in Fig. 3. As one can see from the plot, the results are identically the same at the end of the evolution. Formally, it is due to the fact that the viscosity enters the equation with $\dot{R}$, and therefore it is not really a surprise that the dependence on η diminishes when the system approaches the equilibrium.

It is important to emphasize that the large imbalance in Eq. (33) is expressed in terms of a_c, which, by definition, represents the difference between the initial value of $a(t=0)$ and the finite value of $a(t_{\rm dec})$ at decoherence time $t_{\rm dec}$ when the axion field loses its coherence. It does not depend on the rate at which the axion field $\dot{a}(t)$ evolves, as discussed in Appendix D, where corresponding variations are parametrized by parameter s_c. As one can see from Fig. 2, the changes of the parameter s_c do not produce any visible modifications in the final expression for disparity between nuggets and antinuggets.

This is quite typical behavior for all phenomena related to Berry's phase when the effects normally depend on initial and final conditions rather than on specific dynamical properties of the system. The key element in all our discussions in this subsection is that we are interested in the dimensionless ratio (33) between nuggets and antinuggets

[7]To avoid confusion, one should comment here that $a_c(T)$ itself *implicitly* depends on the temperature as the axion dynamics is highly sensitive to the temperature. Our claim on the "independence" on T_0 refers to *explicit* independence of the disparity (33) on T_0. Implicit dependence of (33) on temperature through $a_c(T)$ always remains.

at the end of the evolution, when the sensitivity to all these dimensional parameters diminishes. The adiabatic approximation for the coherent axion field is also an important element in demonstration of this insensitivity of the final formula (33) to the parameters of the system.

B. Survival of the imbalance between nuggets and antinuggets

In the previous subsection, we argued that disparity (33), which is generated during long lasting evolution of the coherent axion field, is not sensitive to the initial conditions nor to the axion mass m_a. In this subsection, we want to argue that the imbalance (33) survives the subsequent evolution of the system at $t > t_{\rm dec}$ after the axion field loses its coherence on the scale of the Universe as defined in Eq. (31); see also footnote 5 with the related comment.

The basic argument is that the intensity of the axion field is drastically diminished after $t_{\rm dec}$. However, the most important fact is not the amplitude of the remaining axion field but rather its decoherence due to the emission of a large number of randomly propagating axions with typical correlation length $\lambda \sim \hbar/(m_a v_a)$ rather than the Universe scale as in case (6). At this moment, the coefficient $a \equiv 0$ in all our previous formulas. However, the previously generated imbalance (33) does not disappear, and it cannot be washed out because the coherent axion field (6) ceases to exist after $t_{\rm dec}$. In other words, the nuggets and antinuggets will continue to interact with the environment by annihilating or accreting the quarks and antiquarks from outside. However, all these processes are not coherent on the scale of the Universe and will equally influence both types of species.

We want to elaborate on another question which was previously mentioned in footnote 6 and related to our technical assumption that $a_c < 1$ during the evolution (20). In this case, our treatment of $a(t)$ as a marginally small correction is justified. However, our approach obviously breaks down when $a(t)$ becomes large. There is nothing wrong in terms of the physics of this evolution with $a(t) > 1$. It is just a technical treatment of the problem which requires extra care.

The increase $a(t) > 1$ with time can be interpreted in terms of the original parameter $A \simeq \Delta\theta/\pi$ from Eq. (17) to become numerically large (close to 1) as a result of the accumulation of this phase during the long lasting influence of the background axion field. As we mentioned in the text, this $U(1)$ phase of the quark field is directly related to the baryon charge; see Ref. [4] for further technical details. When this phase becomes of order 1, the spectrum of states is completely reconstructed, which effectively corresponds to the modification of the boundary conditions when the integer coefficient N in formula (3) is replaced by $(N + 1)$. After removing the integer portion from A to redefine N, the coefficient $A \simeq \Delta\theta/\pi$ from Eq. (17) can be treated as a small parameter again.

In all respects, this procedure is like the conventional treatment of the angular field $\phi(x)$ when $\phi(x)$ makes a full cycle. The complete description of the system is accomplished by representing $\phi(x)$ in terms of the integer number N and fractional portion $0 \le \phi < 2\pi$ as a result of the periodicity of the angular variable $\phi(x)$. If variable $\phi(x)$ corresponds to a quantum field in quantum field theory (QFT) supporting the topological solitons, this analogy becomes very precise as parameter N corresponds to a specific soliton sector in this QFT model. The fractional portion $\Delta\theta/\pi$ corresponds to the so-called fractionally charged soliton, which is a well-known construction in QFT; see e.g., Ref. [4] with references on the original literature in the given context.

For our specific problem on the imbalance between nuggets and antinuggets, one should emphasize that the disparity (33) holds irrespectively of the behavior $a(t)$ during the evolution. If $a(t)$ becomes large at some moment of the evolution, the corresponding portion of $a(t)$ counts as a conventional baryon charge N in formula (3), which obviously produces an additional imbalance between different species.

To summarize this section, our main claim here is that the results obtained above (showing the disparity between nuggets and antinuggets) are very robust in the sense that they are not very sensitive to the parameters of the theory, such as the axion mass m_a or the misalignment angle θ_0. Furthermore, these results are not very sensitive to the detailed behavior of the system. We also argued that the generated imbalance cannot be washed out by the consequent evolution of the system. Therefore, the computations of the present work strongly support the assumption (8), which is essentially equivalent to Eq. (1), which is a generic consequence of the framework.

V. CONCLUSION AND FUTURE DEVELOPMENT

This work is a natural continuation of the previous studies [4]. The crucial element which was postulated there (without much computational support) is represented by Eq. (8). In the present work, we investigate the evolution of domain-wall bubbles in the presence of a coherent $\mathcal{CP}$-odd axion field. We conclude that the coupling with the coherent axion eventually leads to significant disparity (33) in size between the quark and antiquark nuggets. This provides an essential numerical and analytical support of Eq. (8). We summarize the main results and assumptions of present work as follows:

(1) We assume the PQ transition happens before (or during) the inflation, such that the vacuum is unique and the axion field θ is correlated on the scales of the entire Universe. While the domain walls with $N_{\rm DW} > 1$ cannot be formed in this case, the so-called $N_{\rm DW} = 1$ domain walls, interpolating between one and

the same physical vacuum, still can be formed, as argued in Ref. [4]. This option has been overlooked somehow in previous studies because it had been previously assumed that the all types of the domain walls cannot be formed if the PQ transition happens before the inflation. This element plays a key role in our analysis because the $\mathcal{CP}$-odd axion field is coherent on enormous scales of the entire Universe when the $N_{\rm DW}=1$ domain-wall bubbles can be also formed.

(2) In the presence of a global coherent axion field θ, we argued that a significant disparity (33) between nuggets and antinuggets will be generated. In other words, we argued that the baryon charges separation effect inevitably occurs as a result of the mere existence of the coherent axion field in the early Universe. These studies essentially represent an explicit analytical and numerical support of the basic assumption (8), which is equivalent to the fundamental consequence of the framework (1).

(3) The accumulated disparity (33) is insensitive to the initial conditions, such as θ_0 and T_0, and to the parameters of the system such as the axion mass m_a, as argued in Sec. IV A.

(4) Furthermore, the imbalance (33) between nuggets and antinuggets is not very sensitive to many dynamical parameters of the system. Rather, it is only sensitive to initial and final values of the axion field when it starts to tilt at $t=0$ and loses its coherence at moment $t=t_{\rm dec}$, as argued in Sec. IV B; see also the relevant comment in footnote 5. Such behavior is, in fact, a typical manifestation of the accumulated Berry's phase in condensed matter physics. We also argued in Sec. IV B that the subsequent evolution of the system cannot wash out the previously generated imbalance between nuggets and antinuggets.

(5) We avoid any fine-tuning problems as a result of the features of the system listed in items 3 and 4 above. It further supports our basic claim that the ratio $\Omega_{\rm dark}\approx\Omega_{\rm visible}$ is a very natural and universal outcome of this framework as both types of matter (DM and visible) are proportional to a single dimensional parameter of the system, $\Lambda_{\rm QCD}$. This claim is not sensitive to any specific details of the system.

(6) The baryogenesis in this framework is replaced by the "charge separation" effect as reviewed in Ref. [4]. All criteria but one, Sakharov's criteria [51], are present in our framework (with exception of an explicit baryon charge violation). Indeed, the $\mathcal{C}$ *symmetry* is broken spontaneously on the scale of an individual nugget when the chemical potential μ (which is an odd value under the $\mathcal{C}$ transformation) is locally generated, as explained in Sec. II B. The $\mathcal{CP}$ *symmetry* is broken globally as a result of the coherent axion field (which is odd under $\mathcal{CP}$ transformation), which generates the imbalance (33) between nuggets and antinuggets as highlighted in Sec. II E and explained in great details in the present work. The generated disparity (33) cannot be washed out at the later times as a result of the *nonequilibrium* dynamics when the (originally coherent) axion field produces a large number of random DM axions and loses its coherence at time $t_{\rm dec}$ as explained in Sec. IV B.

We want to conclude with few additional thoughts on the future directions within the framework advocated in present work.

It is quite obvious that a much deeper understanding of the QCD phase diagram at $\theta\neq 0$ is essential for any future progress; see Fig. 1. Due to the known "sign problem," the conventional lattice simulations cannot be used at $\theta\neq 0$. The relevant recent studies [32,52–55] use a number of "lattice tricks" to evade the sign problem. Still, the problem with a better understanding of the phase diagram at $\theta\neq 0$ remains.

Another problem which is worth mentioning is related to a deeper understanding of the formation of closed domain-wall bubbles. Presently, very few results are available on this topic. The most relevant for our studies is the observation made in Ref. [11] that a small number of closed bubbles are indeed observed in numerical simulations. However, their detailed properties (their fate, size distribution, etc.) have not been studied yet. A number of related questions such as an estimation of correlation length $\xi(T)$, the generation of the structure inside the domain walls, the baryon charge accretion on the bubble, etc., can hopefully also be studied in such numerical simulations.

One more possible direction for future studies from the "wish list" is a development of the QCD-based technique related to the evolution of the nuggets, cooling rates, evaporation rates, annihilation rates, viscosity, transmission/reflection coefficients, etc., in an unfriendly environment with nonvanishing T, μ, θ. All these and many other effects, in general, equally contribute to our parameters like $T_{\rm form}$ and $c(T)$ at the $\Lambda_{\rm QCD}$ scale in strongly coupled QCD. Precisely these numerical factors eventually determine the coefficients in the observed relation Eq. (1).

One more possible direction for future studies from the wish list is the improvement of our current understanding by including the CS gap in computations of the nugget's evolution. Such an inclusion can result in a much more precise restriction on the phenomenological parameter $c(T)$ in Eq. (8) relating the baryon to nugget ratio (10).

As we mentioned in Sec. I, this model is consistent with all known astrophysical, cosmological, satellite, and ground-based constraints. The same (anti)nuggets are also the source for the solar neutrino emissions. A very modest improvement in the solar neutrino detection may also lead

to a discovery of the nuggets; see the recent paper [56]. One can also argue that the same (anti)nuggets may explain the long standing problem of the extreme UV and soft x-ray emission from the Solar corona [57].

Last but not least, the discovery of the axion would conclude a long and fascinating journey of searches for this unique and amazing particle conjectured almost 40 years ago; see the recent reviews [9–16] and recent proposal [58] on the axion search experiment which is sensitive to the axion amplitude θ itself, in contrast with conventional proposals which are sensitive to $\dot{\theta}$.

If the PQ symmetry is broken before or during inflation (which is assumed to be the case in our framework as stated in item 1 at the beginning of this section), then a sufficiently large axion mass $m_a \gtrsim 10^{-4}$ eV is unlikely to saturate the dark matter density observed today. Indeed, in this case, the corresponding contribution to $\Omega_{\rm dark}$ resulting from the misalignment mechanism [48] is given by (see e.g., the review [15])

$$\Omega_{\rm axion} \simeq \left(\frac{6\cdot 10^{-6}\ {\rm eV}}{m_a}\right)^{\frac{7}{6}}. \tag{34}$$

This formula essentially states that the axion of mass $m_a \simeq 2\cdot 10^{-5}$ eV saturates the dark matter density observed today, while the axion mass in the range of $m_a \gtrsim 10^{-4}$ eV contributes very little to the dark matter density. Formula (34) accounts only for the axions directly produced by the misalignment mechanism and neglects the axions produced as a result of decay of the topological defects, which becomes the dominant mechanism if the PQ phase transition occurs after the inflation.[8]

In the present work, we advocate the idea that, even if $m_a \gtrsim 10^{-4}$ eV is large and the PQ symmetry is broken before or during inflation, still there is another complementary mechanism contributing to $\Omega_{\rm dark}$ due to the "quark nuggets" formation. We argue that precisely this novel additional mechanism could provide the principle contribution to dark matter of the Universe as the relation $\Omega_{\rm dark} \sim \Omega_{\rm visible}$ in this framework is not sensitive to the axion mass m_a nor to the misalignment angle θ_0 as advocated in the present work.

ACKNOWLEDGMENTS

This work was supported in part by the National Science and Engineering Research Council of Canada.

[8]There is a number of uncertainties and remaining discrepancies in the corresponding estimates. We shall not comment on these subtleties by referring to the original papers [38,45–47]. According to these estimates, the axion contribution to $\Omega_{\rm dark}$ as a result of decay of the topological objects can saturate the observed DM density today if the axion mass is in the range $m_a \sim 10^{-4}$ eV.

APPENDIX A: COHERENT AXION FIELD (6) AS BERRY'S PHASE

In this Appendix, we shall argue that the tiny phase difference proportional to $\theta(t)$ for quarks and antiquarks trapped inside the nuggets and antinuggets might be interpreted as Berry's phase for the Fermi fields. These tiny changes lead to small differences in every individual QCD process as shown in Sec. III. However, these small variations are eventually translated into a large accumulated effect expressed in terms of global properties of the nuggets and antinuggets (such as their typical sizes). This large effect formally expressed as (8) is the direct consequence of the very long lasting accumulation of these tiny $\mathcal{CP}$-odd effects due to the fundamental coherent axion $\theta(t)$ field. Eventually, the generation of $|c(T)| \sim 1$ leads to the model-independent prediction of this framework expressed as (1).

The results of this adiabatic evolution are not sensitive to the parameters of the system but rather sensitive to the initial and final configurations of the system. Such behavior is very typical for many phenomena related to the accumulation of Berry's phase in condensed matter physics when the effects are sensitive to the global rather than local characteristics of the system. Therefore, it is quite natural to expect that the behavior of our system described in Secs. III and IV can be also interpreted as a result of accumulation of Berry's phase which can be identified with the axion background field (6).

Our starting point is the θ term in the QCD Lagrangian $\mathcal{L}_\theta$ where $\theta(t)$ in this work is identified with the axion field

$$\mathcal{L}_\theta = -\theta(t)\frac{g^2}{32\pi^2}\tilde{G}^a_{\mu\nu}G^a_{\mu\nu}. \tag{A1}$$

As is well known, one can rotate the θ term away by rotating the quark fields. Assuming that we have N_f light quarks with equal small masses, one can represent this $U(1)_A$ chiral rotation in the path integral formulation as follows:

$$\psi \to \exp\left(-i\gamma_5\frac{\theta(t)}{N_f}\right)\psi. \tag{A2}$$

There is a number of important consequences of this transformation. We want to mention here just few of them.

First of all, the phase (A2) can be interpreted as Berry's phase, which is coherently accumulated by all quark fields in the entire Universe as long as the field $\theta(t)$ given by (6) is coherent. This phase is obviously numerically much smaller than conventional phases related to the QCD fluctuations which are normally of order $\Lambda_{\rm QCD}$. However, the most important feature of this phase is that it is coherent on the scale of the entire Universe and can be accumulated during a long period of time $\sim m_a^{-1}(t)$, much longer than typical QCD processes with typical time scales $\sim\Lambda_{\rm QCD}^{-1}$.

Berry's phase entering (A2) can be interpreted as a result of the acting of an auxiliary (fictitious) magnetic field in the Hamiltonian $H_{\rm Berry} = \vec{\sigma}\cdot\vec{B}_{\rm Berry}$ where the so-called Berry's curvature $\vec{B}_{\rm Berry}$ assumes the form

$$\vec{B}_{\rm Berry} \sim (m\cos\theta, m\sin\theta, \dot{\theta}). \tag{A3}$$

The parameter m enters the effective Lagrangian (13) and has a physical meaning of a QCD scale as explained in the text. The additional term $\sim\dot{\theta}$ in Eq. (A3) is a result of the $U(1)_A$ chiral rotation (A2) in the path integral when the parameter of the rotation $\theta(t)$ depends on time. The corresponding Lagrangian generating this term has the form $\mathcal{L}_5 = \dot{\theta}\bar{\psi}\gamma_0\gamma_5\psi$. The $\dot{\theta}$ in this expression can be interpreted as axial chemical potential $\mu_5 = \dot{\theta}$, which normally enters the Lagrangian as $\mathcal{L}_5 = \mu_5\bar{\psi}\gamma_0\gamma_5\psi$.

In writing down an explicit expression for Berry's curvature $\vec{B}_{\rm Berry}$, we used a specific frame determined by γ_μ- representation as given in Ref. [4]. In this representation, the auxiliary Berry's curvature $\vec{B}_{\rm Berry}$ can be thought of as a vector rotating along the equator in the xy plane (neglecting the small $B^z_{\rm Berry}\sim\dot{\theta}$ component) in this specific frame when time evolves. It is important to emphasize that this auxiliary field never returns to its original position after a complete cycle because the axion field reduces its amplitude during the evolution. The corresponding energy of the coherent axion field eventually goes to the production of the propagating dark matter axions as a result of the conventional misalignment mechanism. After the energy of the original field (6) is transferred to the propagating axions, the large scale coherence (with the size of the Universe) is lost, and the typical coherence length is determined by λ_D, which is a much smaller scale.

The idea that the axion field can be thought of as an auxiliary (fictitious) magnetic field is not a new idea and has been discussed in a number of papers in the past; see e.g., recent articles [18,22,25,28] devoted to the axion search experiments. A novel element advocated in the present work is that this field (6) is coherent on enormous scales of the Universe before it decays to the propagating dark matter axions.

Another important consequence of the accumulated phase (A2) is that the ground state (the QCD vacuum) in the background of the coherent axion field (6) explicitly violates $\mathcal{CP}$ invariance as can be explicitly seen by computing the $\langle\det\bar{\psi}^f_L\psi^f_R\rangle$; see below. The corresponding computations can be carried out in a theoretically controllable way at sufficiently high temperature $T > T_c$ when the instanton approximation is justified. This region of temperatures is precisely when the domain-wall network only starts to form and the axion field just starts to roll.

The corresponding technical computations are well known and presented in Appendix B,

$$\langle\det\bar{\psi}^f_L\psi^f_R\rangle \sim e^{i\theta(t)}\cdot\Lambda^{3N_f}_{\rm QCD}\left(\frac{\Lambda_{\rm QCD}}{T}\right)^{\frac{11}{3}(N-N_f)}, \tag{A4}$$

where f stands for the flavor of a light quark. A few comments about this important formula are in order. First of all, the vacuum condensate (A4) does not vanish even in the deconfined phase (well above the transition at $T \gg T_c$ shown on Fig. 1), in the region where the chiral symmetry is restored and the chiral condensate itself vanishes, i.e., $\langle\bar{\psi}\psi\rangle = 0$. This is because the vacuum condensate (A4) is formed due to the explicit violation of the $U(1)_A$ symmetry rather than due to spontaneous $SU(3)_L\times SU(3)_R$ chiral symmetry. Furthermore, $\langle\det\bar{\psi}^f_L\psi^f_R\rangle$ does not vanish in the chiral limit $m_q\to 0$; see discussions in Appendix B.

Another important comment is that formula (A4) is derived in the dilute instanton gas approximation, which is known to become a theoretically justifiable approximation at sufficiently high temperature of order a few times $\Lambda_{\rm QCD}$; see the detailed discussions on this matter in Appendix B. An important comment we would like to make here is that the decreasing of the condensate (A4) with increasing the temperature is much slower than in the case of topological susceptibility $\chi(T)\sim f_a^2 m_a^2(T)$ which determines the axion mass dependence on temperature $m_a(T)$; see recent numerical studies in Refs. [30–33].

Furthermore, the condensate (A4) also depends on the chemical potential [not shown explicitly in estimate (A4) to simplify notations]; see Appendix B with relevant comments. This feature has an important implication for our discussions in Secs. III and IV as the μ dependence of the vacuum condensate (A4) implies that the ground states inside and outside the nuggets would be different.

The key element for the present work is that the vacuum condensate (A4) explicitly depends on the axion phase $\theta(t)$ as a result of $U(1)_A$ transformation (A2). The presence of this phase unambiguously implies that the ground state violates $\mathcal{CP}$ invariance even in the deconfined quark-gluon plasma well above the transition temperature T_c. This $\mathcal{CP}$ violation occurred when $T > T_c$, which happens long before the axion field settles down at the origin $\theta = 0$ when the chiral phase transition occurs at $T \simeq T_c$. This remark has some profound cosmological consequences discussed in the main text in Secs. III and IV as the phase (6) is correlated on enormous scales at this early stage of evolution.

APPENDIX B: COMPUTATIONS OF THE $\langle\det\bar{\psi}^f_L\psi^f_R\rangle$

The main goal of this Appendix is to derive formula (A4) for the vacuum expectation value $\langle\det\bar{\psi}^f_L\psi^f_R\rangle$ in the deconfined phase where the instanton base computations are under complete theoretical control for sufficiently large T, which is precisely the region where the axion field starts to roll and the domain-wall network starts to form. In the

context of the present work, the generation of this condensate unambiguously implies that the ground state is $\mathcal{P}$ and $\mathcal{CP}$ odd as a result of the axion field θ given by (6), which is coherent on an enormous scale at this period of the time evolution. One should emphasize that the θ dependence enters through the nonperturbative dynamics in the deconfined regime. As is well known, the θ dependence cannot enter the dynamics on the level of perturbation theory.

We use the standard formula for the instanton density at one-loop order [59–61],

$$n(\rho) = C_N(\beta(\rho))^{2N}\rho^{-5}\exp[-\beta(\rho)] \times \exp\left[-\left(N_f\mu^2 + \frac{1}{3}(2N+N_f)\pi^2T^2\right)\rho^2\right], \quad \text{(B1)}$$

where

$$C_N = \frac{0.466e^{-1.679N}1.34^{N_f}}{(N-1)!(N-2)!},$$
$$\beta(\rho) = -b\log(\rho\Lambda_{\rm QCD}), \qquad b = \frac{11}{3}N - \frac{2}{3}N_f.$$

This formula contains, of course, the standard instanton classical action $\exp(-8\pi^2/g^2(\rho)) \sim \exp[-\beta(\rho)]$ which, however, is hidden as it is expressed in terms of $\Lambda_{\rm QCD}$ rather than in terms of coupling constant $g^2(\rho)$. This nonanalytical dependence $\exp(-8\pi^2/g^2)$ explicitly shows the nonanalytical and nonperturbative nature of the condensate $\langle\det\bar\psi^f_L\psi^f_R\rangle$ to be computed below based on expression (B1).

We inserted the chemical potential $\mu = \mu_B/N$ along with temperature T into this expression to demonstrate that the instanton density becomes exponentially small for sufficiently large T, which explains the justification of the dilute instanton gas approximation in this regime.

The computation of condensate $\langle\det\bar\psi^f_L\psi^f_R\rangle$ is reduced to the following expression,

$$\langle\det\bar\psi^f_L\psi^f_R\rangle = e^{i\theta(t)}\int d\rho n(\rho)d^4x\prod_i^{N_f}\frac{2\rho^3}{\pi^2[x^2+\rho^2]^3}, \quad \text{(B2)}$$

where we keep only zero modes in the chiral limit,[9] assuming that in the dilute gas approximation (which is justified for sufficiently large T as we mentioned above) all other mode contributions are suppressed by factor $m_q \to 0$. The integration over d^4x corresponds to the integration over the instanton center at point x.

[9]It is known that the zero modes explicitly depend on the chemical potential; see e.g., the review [61]. We neglect these minor corrections for our estimates in the present work.

The important point here is that the axion field θ explicitly enters the expression (B2), such that the condensate violates $\mathcal{P}$ and $\mathcal{CP}$ symmetries in the ground state. Another important comment is that the integral $\int d\rho$ is convergent, and for sufficiently large T, the expression (B2) represents the dominant contribution for this nonperturbative vacuum condensate. It is important to emphasize that the condensate $\langle\det\bar\psi^f_L\psi^f_R\rangle$ does not vanish[10] in the chiral limit $m_q \to 0$, in contrast with the partition function itself, $\mathcal{Z}$, which vanishes as $\mathcal{Z} \sim m_q^{N_f}$. The topological susceptibility $\chi \sim \partial^2\mathcal{Z}/\partial\theta^2$ as well as the axion mass $m_a^2 \sim \chi \sim m_q^{N_f}$ also vanish in the chiral limit.[11]

After integration over d^4x, one arrives at the following expression,

$$\langle\det\bar\psi^f_L\psi^f_R\rangle = \frac{\pi^2\cdot e^{i\theta(t)}}{(3N_f-1)(3N_f-2)}\int d\rho n(\rho)\rho^4\left(\frac{2}{\pi^2\rho^3}\right)^{N_f},$$

where $n(\rho)$ is defined as before by Eq. (B1). The combination $\int d\rho n(\rho)\rho^4$ is dimensionless, while the dimension of the operator $\langle\det\bar\psi^f_L\psi^f_R\rangle \sim \langle\rho\rangle^{-3N_f} \sim ({\rm MeV})^{3N_f}$ as it should. After integration over the instanton sizes $d\rho$, one arrives at

$$\langle\det\bar\psi^f_L\psi^f_R\rangle \sim e^{i\theta(t)}\Lambda_{\rm QCD}^{3N_f}\left(\frac{\Lambda_{\rm QCD}}{T}\right)^{\frac{11}{3}(N-N_f)}, \quad \text{(B3)}$$

where for simple estimates we neglect all $(\log\rho)^n$ and all numerical factors in the integrand as they do not play any essential role in the present work. This formula is precisely the expression (A4) we used in the previous Appendix.

APPENDIX C: TECHNICAL DETAILS

This Appendix is devoted to the derivation of the pressure term given by Eq. (23). It plays an important role in our analysis in Sec. III B. The basic idea is to use the net baryon charge conservation given by in Eq. (21) and relate the radius of a domain-wall bubble to its chemical potential, similar to the procedure we used in our previous studies in Ref. [4]. The new element now is the extra term $\sim a$ due to the background axion filed, which has different signs for the nuggets and antinuggets. The relevant formula reads

[10]In fact, this unique feature for this condensate $\langle\det\bar\psi^f_L\psi^f_R\rangle$ in the chiral limit motivated a proposal to view the vacuum condensate $\langle\det\bar\psi^f_L\psi^f_R\rangle$ as an order parameter to study the phase transition to the conformal window in the limit of large N and finite $N_f/N \sim 1$; see Ref. [62] for references and details.

[11]At low temperatures $T \simeq 0$, the corresponding features are quite different because the chiral condensate $\langle\bar\psi^f_L\psi^f_R\rangle \neq 0$ and also because in the $U(1)_A$ channel there are no massless degrees of freedom as the η' is a massive state.

$$x^2 \simeq \left(\frac{T_0}{T}\right)^2 \frac{I_2^{(\pm)}(0)}{I_2^{(\pm)}(b)}\left[1 \mp \frac{AR_0T}{3\pi}x \cdot \frac{I_3^{(\pm)}(b)}{I_2^{(\pm)}(b)}\right] \simeq \left(\frac{T_0}{T}\right)^2 \frac{I_2^{(\pm)}(0)}{I_2^{(\pm)}(b)}\left[1 \mp \frac{2}{3}ax\left(\frac{3}{2}+\frac{2}{3}\sqrt{I_2^{(\pm)}(b)}\right)\right], \tag{C1}$$

where $x = R/R_0$, and $a = AR_0T/2\pi$ as defined in Eq. (20). In the second step, we use the approximated relation $I_3(b)/I_2(b) \simeq \frac{3}{2} + \frac{2}{3}\sqrt{I_2(b)}$; see Appendix E.

Our next step is to approximate and simplify $I_2^{(\pm)}(b)$ by expanding it with respect to small parameter a. We keep the linear terms only as a is assumed to be a numerically small parameter, i.e.,

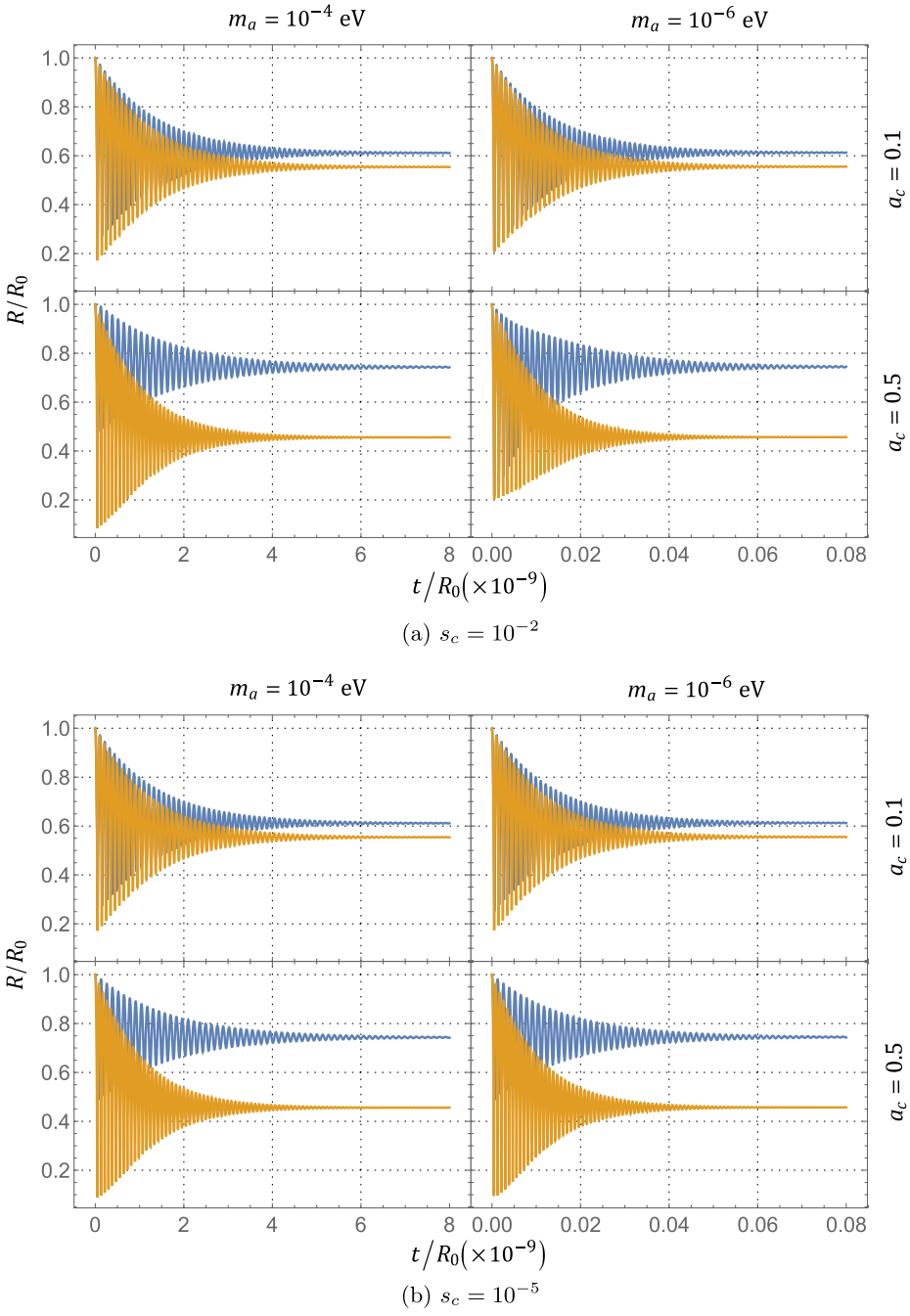

(a) $s_c = 10^{-2}$

(b) $s_c = 10^{-5}$

FIG. 2. Numerical solutions of (anti)nuggets evolving in the background of axion field before QCD transition. The blue and orange lines represent the evolutions of $R^-(s)$ and $R^+(s)$, respectively. We plot the upper four subfigures in (a) with $s_c = 10^{-2}$ and the lower four subfigures in (b) with $s_c = 10^{-5}$. The numerical values of parameters m_a and a_c that we use in calculating each subfigure can be seen in the upper edge and right edge of the graph.

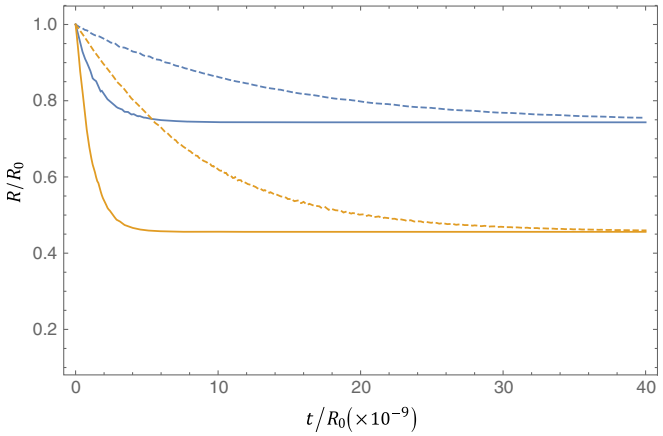

FIG. 3. Dependence on viscosity η. Amplitudes of R^- (blue) and R^+ (orange) are plotted. The solid lines correspond to $\eta = 8.4 m_\pi^3 (\times 10^9)$, and the dashed lines correspond to $\eta = 1.0 m_\pi^3 (\times 10^9)$. Here, parameters $m_a = 10^{-4}$ eV and $s_c = 10^{-5}$ are chosen.

$$I_2^{(\pm)}[b(R)] \simeq \left(\frac{T_0}{T}\right)^2 \frac{I_2(0)}{x^2}\left[1 \mp \left(\frac{4}{9}\frac{T_0}{T}\sqrt{\frac{\pi^2}{12}+x}\right)a\right] \equiv f^{(\pm)}(R). \tag{C2}$$

We introduce special notations for this combination of (R, a, T) by introducing a function $f^{(\pm)}(R)$, which enters formula Eq. (23) in the main text. This function is very useful because every higher order Fermi integral $I_n(b)$ (and some simple polynomial functions) can be well approximated in terms of the function of $I_2(b)$; see Appendix E. This property allows us to rewrite all terms of chemical potential $b = |\mu|/T$ into a simple function of radius R using the relation (C2).

To conclude this Appendix, we want to alert the readers that the definition of $f^{(\pm)}(R)$ introduced above is slightly different from $f(R)$ introduced in our previous work [4]. While the two functions play a similar role in the analysis, they are not identically the same even in the limit $a = 0$. In the present work, $f^{(\pm)}(R)$ is defined as $I_2[b(R)]$, while in the previous work, it is defined as $f(R) \equiv I_2[b(R)] - \pi^2/6$. We opted to use a new definition (C2) in the present work because it produces much better accuracy with the approximations and simplifications for the Fermi integrals adopted in the present work. In fact, the accuracy of the present work is order $\pm 5\%$, which should be compared with typical accuracy $\sim 20\%$ from the previous work [4] when similar approximations are made.

APPENDIX D: NUMERICAL RESULTS SUPPORTING (33)

Our goal here is to solve Eq. (22) without using a large number of simplifications and approximations of Sec. III. Let us remind the reader that the goal of Sec. III was to make a qualitative analysis leading to (33), rather than a precise quantitative description. In this Appendix, we use the exact form of Fermi integrals. In addition, we also keep the contribution $\sim E_B \theta(b - b_1)$ in (23), which was neglected in our qualitative analysis in Sec. III.

Furthermore, as we mentioned in Sec. III B, we use the adiabatic approximation in the computations of the nugget's dynamics (oscillations with slow damping). This adiabatic approximation is technically achieved by assuming that $m_a(T)$ and T are the constants in the course of computations. This assumption can be only justified if the typical time scales of the relevant processes such as nugget's oscillations are much shorter than the time scale when the external parameters $[\theta(T), m_a(T), T]$ vary. To justify our approximation, we compute the ratio ω_R/ω_θ. In this formula, ω_R represents a typical frequency of the nuggets oscillation, while ω_θ represents the frequency of oscillations of the axion field.

The computation of $\omega_\theta \simeq m_a$ is based on the interpolation formula (between low and high temperatures) for the topological susceptibility derived in Ref. [44]:

$$m_a^2 f_a^2 = 1.46 \times 10^{-3} \frac{\Lambda^4 (1 + 0.5\frac{T}{\Lambda})}{1 + (3.53\frac{T}{\Lambda})^{7.48}}, \quad \Lambda \simeq 0.4 \text{ GeV}. \tag{D1}$$

It is known that this expression deviates from the lattice results [30–33]. Nevertheless, it obviously reflects all the crucial elements in the behavior of the topological susceptibility and the axion mass $m_a(T)$ as a function of the temperature T. It is certainly a sufficiently good approximation for our qualitative estimates of the ratio ω_R/ω_θ.

The computation of ω_R is based on the numerical solution[12] of Eq. (22) for a few consecutive oscillations of $R(t)$ for different values of the temperature $170 \text{ MeV} \le T \le 500 \text{ MeV}$. The corresponding ratio $\omega_R(T)/\omega_\theta(T)$ as a function of the temperature is shown on Fig. 4. The most important lesson from these computations is that this ratio is always much larger than unity, even in the vicinity of the chiral phase transition at $T \simeq 170$ MeV when the chiral condensate forms and the axion mass assumes its final maximum value. This estimate unambiguously implies that our adiabatic approximation is justified as the nuggets make a large number of oscillations, while the axion field varies only slightly as the relation $\omega_R \gg \omega_\theta$ states.

As we shall see below, the numerical studies of this Appendix strongly support the qualitative analysis presented in Sec. III and specifically the basic result (33)

[12]In the corresponding numerical computations, we do not assume the smallness of the oscillations. Therefore, we do not use expansion around the minimum of the potential leading to approximate linearized equation (26).

demonstrating the disparity between nuggets and antinuggets due to the interaction with the coherent axion field.

The parameter $a(t)$ was introduced in Eq. (20) to describe the accumulation of $\mathcal{CP}$-odd effects as the result of the evolution of the nuggets in the background of axion field. As discussed in Sec. III B, $a(t)$ is a monotonically increasing function of time. Essentially, this behavior corresponds to the axion potential, which becomes more and more tilted with time as the axion mass $m_a(T)$ is increasing when the temperature slowly approaches the transition value T_c from above. When the axion potential becomes more tilted, the corresponding rate of the axion's emission also increases. It obviously leads to the decay of the axion amplitude θ as the energy from the coherent axion field (6) is transferred to the propagating axions. This effect of the diminishing of the axion field is parametrized by A in Eq. (17), which precisely describes the decreasing of the axion amplitude during a single cycle. At some moment $t_{\rm dec}$ in this evolution, the axion field loses its coherence approaching its critical value a_c as described in the text; see Eq. (31) and footnote 5. At this moment, the axion field may still produce the axions, but it cannot lead to any coherent (on the scale of the Universe) changes such as (33).

In the numerical studies below, we concentrate only on computation of the disparity (33), while the background approximation (20) remains valid. The generalization of this result on the case when the critical value a_c becomes large is straightforward and discussed in Sec. IV B.

Therefore, we model $a(t)$ to be increasing with time from zero and (smoothly) stopping at some cutoff value $a_c \leq 1$ corresponding to the decoherence moment $t_{\rm dec}$, i.e.,

$$a(s) = a_c \tanh\left(\frac{s}{s_c}\right), \qquad s \equiv t/R_0, \tag{D2}$$

where a_c and s_c serve as two free parameters. For convenience in numerical computation, we use the "rescaled" time $s \equiv t/R_0$ in this Appendix. The parameter a_c is defined by (31) and corresponds to the moment when the axion field loses its coherence as explained above and in footnote 5. The parameter s_c describes the rate at which the parameter $a(t)$ changes with time.

As manifested in numerical evaluation, the final effects of the disparity (33) do not depend on what the exact model for $a(t)$ is. More specifically, the rate of the variation of $a(t)$ does not affect the final magnitude of the disparity between two species. Here, we model it as the hyperbolic tangent form just for the convenience of numerical calculations. In the model (D2), we describe the critical point using the cutoff a_c. As one can see from Fig. 2, the final disparity effects do not depend on parameter s_c but only depend on the value of a_c when the coherence of the axion field is lost. Figure 2 also shows that the disparity effects do not depend on the axion mass m_a, in agreement with our arguments in Sec. IV A.

TABLE I. Table for some numerical parameters.

Quantity	Value	QCD units ($m_\pi = 1$)
Flavors N_f	2	2
Colors N_c	3	3
Degeneracy factor (in) $g^{\rm in}$	12	12
Degeneracy factor (out) $g^{\rm out}$	37	37
Bag constant E_B	$(150\ \text{MeV})^4$	1.5
"Squeezer" parameter μ_1	330 MeV	2.4
Initial temperature T_0	200 MeV	1.5
QCD viscosity η [63,64]	$0.002\ \text{GeV}^3$	1
QCD viscosity η [65]	$0.02\ \text{GeV}^3$	8.4
Axion decay constant f_a	10^{10} GeV	7.4×10^{10}
Mass of axion m_a	10^{-4} eV	7×10^{-13}
Mass of axion m_a	10^{-6} eV	7×10^{-15}
Domain-wall tension $\sigma(m_a \sim 10^{-4}\ \text{eV})$	$9 \times 10^5\ \text{GeV}^3$	3.7×10^8
Domain-wall tension $\sigma(m_a \sim 10^{-6}\ \text{eV})$	$9 \times 10^7\ \text{GeV}^3$	3.7×10^{10}
Initial radius $R_0 \sim m_a^{-1}$	0.2 cm	1.4×10^{12}
Initial radius $R_0 \sim m_a^{-1}$	20 cm	1.4×10^{14}

The disparity effects also do not depend on the viscosity η. To support this claim, we did two different computations with different values of viscosity. The first choice was motivated by our previous studies [4] where we used $\eta \simeq m_\pi^3$, which has been computed in different models under different conditions in Refs. [63,64]. It is known that the viscosity is in fact is somewhat larger in the region of sufficiently high temperature. Therefore, for the second choice, we use the holographic arguments of Ref. [65], suggesting that η could be 1 order of magnitude larger than conventional perturbative QCD predictions (we use factor 8.4 in our numerical computations). One can explicitly see from Fig. 3 that the final destination for the disparity effects does not depend on the viscosity, in agreement with the general arguments of Sec. IV A.

We summarize the numerical values of other parameters and constants needed in calculations in Table. I. We choose initial temperature T_0 as 200 MeV. The (anti)nuggets evolve in the background axion field from 200 MeV to the QCD transition temperature 170 MeV, and we can safely take the temperature as a constant, $T/T_0 \simeq 1$.

In Fig. 2(a), we draw 2×2 subfigures,[13] for $m_a \simeq (10^{-4}, 10^{-6})$ eV, $a_c = (0.1, 0.5)$, and we set the

[13]To make the numerical computations solvable and the pattern of oscillations in Fig. 2 visible, here we adopt the rescaled QCD viscosity $\tilde{\eta} = 10^9\eta$, following Ref. [4]. This will not change any important results that we care about, like the formation radius of (anti)nuggets $R^{\pm}_{\rm form}$. The advantage is that this adoption will greatly "shorten" the evolution time and therefore make the numerical computations feasible. Correspondingly, we add an extra factor 10^{-9} in the horizontal label in Fig. 2. Otherwise, if we directly use the value of η, Fig. 2 should be 9 orders of magnitude longer than shown.

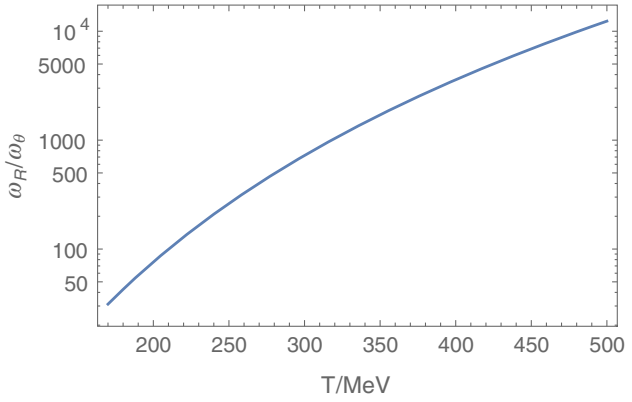

FIG. 4. This plot shows that ω_R/ω_θ is always much larger than unity. This behavior justifies our adiabatic approximation in numerical analysis when the axion mass $m_a(T)$ and the axion field $\theta(T)$ are kept constant. This plot essentially shows that the nuggets make a very large number of oscillations, while the axion field $\theta(T)$ slowly varies.

parameter $s_c = 10^{-2}$. We set the viscosity as $\eta = 8.4m_\pi^3$. Figure 2(b) is the same as the Fig. 2(a) but with a different parameter $s_c = 10^{-5}$. The blue and orange lines represent the evolution of $R^-(s)$ and $R^+(s)$, respectively. The difference between these two kinds of lines is the accumulated disparity effects. Comparing Fig. 2(a) with Fig. 2(b), we see that changing s_c will not affect the disparity effects. This verifies that the difference between two kinds of nuggets is insensitive to how a increases, fast or slow. In Fig. 2(a) or Fig. 2(b), comparing the four subfigures horizontally with a_c fixed and m_a varied, we see that the disparity effects are independent of m_a. This supports the arguments in Sec. IV A that the disparity effects are insensitive to the mass of the axion. Then, we compare the four subfigures vertically with a_c varied and m_a fixed. We see that the disparity effects are determined by a_c rather than other parameters. For $a_c = 0.1$, we see that $\Delta R_{\rm form} = |R^+_{\rm form} - R^-_{\rm form}| \simeq 0.06$ and $\langle R_{\rm form}\rangle = \frac{1}{2}|R^+_{\rm form} + R^-_{\rm form}| \simeq 0.6$,

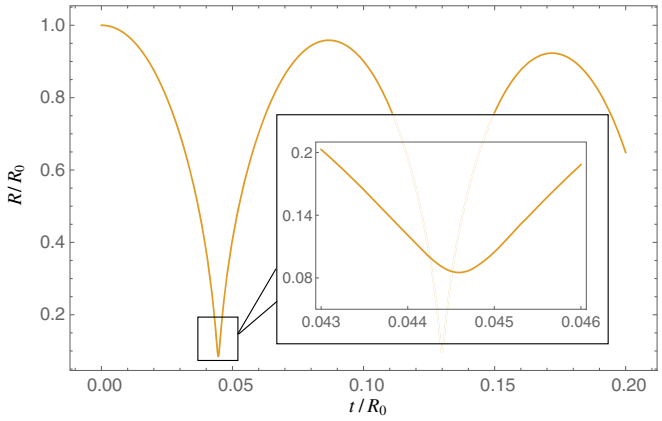

FIG. 5. The first few oscillations of R^+ in the lower left subfigure of Fig. 2. We choose this as an example to show that there is no cuspy problem.

consistent with the analytical relation (32) in Sec. III. For $a_c = 0.5$, $\Delta R_{\rm form} \simeq 0.3$ and $\langle R_{\rm form}\rangle \simeq 0.6$, again consistent with the relation (32).

We also notice that the oscillations shown in Fig. 2 are very sharp. But this seemingly cuspy behavior is in fact quite smooth on the QCD scale. To see this, we zoom in on the first few oscillations of R^+ in the lower left subfigure of Fig. 2(a) and plot this in Fig. 5. We see that the duration of the "cusp" is $\delta t_{\rm cusp} \sim 10^{-3} R_0$, which is much longer than the QCD scale $\delta t_{\rm cusp} \gg \Lambda^{-1}_{\rm QCD}$. One should also add that the oscillation frequency is not sensitive to the viscosity η according to Eq. (27b). Therefore, our comment about "noncuspy" behavior remains unaffected as the time scale of a single oscillation (and therefore $\delta t_{\rm cusp}$) is not sensitive to the viscosity η.

APPENDIX E: FERMI INTEGRALS

We now study some more details on the Fermi integral of the following form:

$$I_n(b) = \int_0^\infty \frac{dx \cdot x^{n-1}}{e^{x-b}+1}. \tag{E1}$$

Such integrals can be exactly solved in terms of the so-called "polylog" function of degree n:

$$\mathrm{Li}_n(z) = \sum_{k=1}^{\infty} \frac{1}{k^n} z^k. \tag{E2}$$

Specifically, we obtain the following exact solution,

$$I_n(b) = -\Gamma(n)\mathrm{Li}_n(-e^b), \tag{E3}$$

where $\Gamma(n)$ is the gamma function. Also, one may find the polylog function satisfies following property when doing derivation:

$$\frac{d}{db}\mathrm{Li}_n(-e^b) = \mathrm{Li}_{n-1}(-e^b). \tag{E4}$$

This property implies a useful relation between different I_n's:

$$\frac{d}{db} I_n(b) = (n-1) I_{n-1}(b). \tag{E5}$$

For $b \geq 0$, we sometimes prefer to approximate $I_n(b)$ in terms of "basic" functions:

$$I_1(b) = \ln(1+e^b) \qquad \text{(exact)} \tag{E6a}$$

$$I_2(b) \simeq \frac{\pi^2}{6} + \frac{1}{2}b^2 - \frac{\pi^2}{12}e^{-b} \qquad (\pm 2\%) \tag{E6b}$$

$$I_3(b) \simeq \frac{\pi^2}{3}b + \frac{1}{3}b^3 + \frac{3}{2}\zeta(3)\cdot e^{-b} \qquad (\pm 2\%) \tag{E6c}$$

$$I_4(b) \simeq \frac{7\pi^4}{60} + \frac{\pi^2}{2}b^2 + \frac{1}{4}b^4 - \frac{7\pi^4}{120}e^{-b} \qquad (\pm 3\%). \quad \text{(E6d)}$$

All approximations are highly accurate within $\pm 3\%$ uncertainty. Other useful approximations can be writing higher order $I_n(b)$ in terms of $I_2(b)$. For examples,

$$\frac{I_3(b)}{I_2(b)} \simeq \frac{3}{2} + \frac{2}{3}\sqrt{I_2(b)} \qquad (\underbrace{\pm 5\%}_{b\lesssim 5}; \underbrace{\pm 10\%}_{b\lesssim 10}). \quad \text{(E7)}$$

Note that $\mu_{\max} \simeq 500$ MeV is the critical upper limit of the QCD cutoff and $T \gtrsim 170$ MeV before QCD transition; thus, $b \lesssim 3$ is the full applicable domain in the present study. A similar approximation for $I_4(b)$ is

$$I_4(b) \simeq 2\pi I_2(b) + (I_2(b))^2 \qquad \underbrace{(\pm 3\%)}_{b\lesssim 10}. \quad \text{(E8)}$$

Also, before transition, $T \gtrsim 170$ MeV. Thus, this approximation is within 5% of error since $b \lesssim 3$. Also, near the transition $T \lesssim 220$ MeV, we can also approximate

$$b^2 \simeq 2.92 + 2I_2(b) \qquad \underbrace{(\pm 3\%)}_{b\gtrsim 1.5}, \quad \text{(E9)}$$

which is a valid approximation for $\mu > \mu_1 \simeq 330$ MeV.

[1] A. R. Zhitnitsky, J. Cosmol. Astropart. Phys. 10 (2003) 010.
[2] D. H. Oaknin and A. Zhitnitsky, Phys. Rev. D **71**, 023519 (2005).
[3] E. Witten, Phys. Rev. D **30**, 272 (1984).
[4] X. Liang and A. Zhitnitsky, Phys. Rev. D **94**, 083502 (2016).
[5] Y. Aoki, G. Endrodi, Z. Fodor, S. D. Katz, and K. K. Szabo, Nature (London) **443**, 675 (2006).
[6] R. D. Peccei and H. R. Quinn, Phys. Rev. D **16**, 1791 (1977); S. Weinberg, Phys. Rev. Lett. **40**, 223 (1978); F. Wilczek, Phys. Rev. Lett. **40**, 279 (1978).
[7] J. E. Kim, Phys. Rev. Lett. **43** (1979) 103; M. A. Shifman, A. I. Vainshtein, and V. I. Zakharov, Nucl. Phys. **B166**, 493 (1980).
[8] M. Dine, W. Fischler, and M. Srednicki, Phys. Lett. **104B**, 199 (1981); A. R. Zhitnitsky, Yad. Fiz. **31**, 497 (1980) [Sov. J. Nucl. Phys. **31**, 260 (1980)].
[9] K. van Bibber and L. J. Rosenberg, Phys. Today **59**, 30 (2006).
[10] S. J. Asztalos, L. J. Rosenberg, K. van Bibber, P. Sikivie, and K. Zioutas, Annu. Rev. Nucl. Part. Sci. **56**, 293 (2006).
[11] P. Sikivie, Lect. Notes Phys. **741**, 19 (2008).
[12] G. G. Raffelt, Lect. Notes Phys. **741**, 51 (2008).
[13] P. Sikivie, Int. J. Mod. Phys. A **25**, 554 (2010).
[14] L. J. Rosenberg, Proc. Nat. Acad. Sci. **112**, 12278 (2015).
[15] P. W. Graham, I. G. Irastorza, S. K. Lamoreaux, A. Lindner, and K. A. van Bibber, Annu. Rev. Nucl. Part. Sci. **65**, 485 (2015).
[16] A. Ringwald, *Proc. Sci.*, NOW2016 (2016) 081.
[17] D. Budker, P. W. Graham, M. Ledbetter, S. Rajendran, and A. Sushkov, Phys. Rev. X **4**, 021030 (2014).
[18] P. W. Graham and S. Rajendran, Phys. Rev. D **88**, 035023 (2013).
[19] G. Rybka, A. Wagner, A. Brill, K. Ramos, R. Percival, and K. Patel, Phys. Rev. D **91**, 011701 (2015).
[20] P. Sikivie, N. Sullivan, and D. B. Tanner, Phys. Rev. Lett. **112**, 131301 (2014).
[21] C. Beck, Phys. Rev. Lett. **111**, 231801 (2013).
[22] Y. V. Stadnik and V. V. Flambaum, Phys. Rev. D **89**, 043522 (2014).
[23] P. Sikivie, Phys. Rev. Lett. **113**, 201301 (2014).
[24] B. T. McAllister, S. R. Parker, and M. E. Tobar, Phys. Rev. Lett. **116**, 161804 (2016); **117**, 159901(E) (2016).
[25] C. T. Hill, Phys. Rev. D **91**, 111702 (2015).
[26] C. T. Hill, Phys. Rev. D **93**, 025007 (2016).
[27] Y. Kahn, B. R. Safdi, and J. Thaler, Phys. Rev. Lett. **117**, 141801 (2016).
[28] R. Barbieri, C. Braggio, G. Carugno, C. S. Gallo, A. Lombardi, A. Ortolan, R. Pengo, G. Ruoso, and C. C. Speake, Phys. Dark Universe **15**, 135 (2017).
[29] A. Arvanitaki and A. A. Geraci, Phys. Rev. Lett. **113**, 161801 (2014).
[30] R. Kitano and N. Yamada, J. High Energy Phys. 10 (2015) 136.
[31] C. Bonati, M. D'Elia, M. Mariti, G. Martinelli, M. Mesiti, F. Negro, F. Sanfilippo, and G. Villadoro, J. High Energy Phys. 03 (2016) 155.
[32] S. Borsanyi, Z. Fodor, J. Guenther, K.-H. Kampert, S. D. Katz, T. Kawanai, T. G. Kovacs, S. W. Mages, A. Pasztor, F. Pittler, J. Redondo, A. Ringwald, and K. K. Szabo, Nature (London) **539**, 69 (2016).
[33] P. Petreczky, H. P. Schadler, and S. Sharma, Phys. Lett. B **762**, 498 (2016).
[34] A. Zhitnitsky, Phys. Rev. D **74**, 043515 (2006).
[35] A. Zhitnitsky, Eur. Phys. J. Web Conf. **137**, 09014 (2017).
[36] P. Sikivie, Phys. Rev. Lett. **48**, 1156 (1982); A. Vilenkin and A. E. Everett, Phys. Rev. Lett. **48**, 1867 (1982).
[37] A. Vilenkin and E. P. S. Shellard, *Cosmic Strings and Other Topological Defects* (Cambridge University Press, Cambridge, England, 1994).
[38] S. Chang, C. Hagmann, and P. Sikivie, Phys. Rev. D **59**, 023505 (1998).
[39] M. M. Forbes and A. R. Zhitnitsky, J. High Energy Phys. 10 (2001) 013.
[40] G. Gabadadze and M. A. Shifman, Phys. Rev. D **62**, 114003 (2000).

[41] D. T. Son, M. A. Stephanov, and A. R. Zhitnitsky, Phys. Rev. Lett. **86**, 3955 (2001).
[42] T. W. B. Kibble, J. Phys. A **9**, 1387 (1976); W. Zurek, Nature (London) **317**, 505 (1985).
[43] W. Zurek, Phys. Rep. **276**, 177 (1996).
[44] O. Wantz and E. P. S. Shellard, Phys. Rev. D **82**, 123508 (2010); Nucl. Phys. **B829**, 110 (2010).
[45] T. Hiramatsu, M. Kawasaki, K. Saikawa, and T. Sekiguchi, Phys. Rev. D **85**, 105020 (2012); **86**, 089902(E) (2012).
[46] M. Kawasaki, K. Saikawa, and T. Sekiguchi, Phys. Rev. D **91**, 065014 (2015).
[47] L. Fleury and G. D. Moore, J. Cosmol. Astropart. Phys. 01 (2016) 004.
[48] J. Preskill, M. B. Wise, and F. Wilczek, Phys. Lett. **120B**, 127 (1983); L. Abbott and P. Sikivie, Phys. Lett. **120B**, 133 (1983); M. Dine and W. Fischler, Phys. Lett. **120B**, 137 (1983).
[49] M. G. Alford, A. Schmitt, K. Rajagopal, and T. Schäfer, Rev. Mod. Phys. **80**, 1455 (2008).
[50] K. Rajagopal and F. Wilczek, arXiv:hep-ph/0011333.
[51] A. D. Sakharov, JETP Lett. **5**, 24 (1967).
[52] M. D'Elia and F. Negro, Phys. Rev. D **88**, 034503 (2013).
[53] C. Bonati, M. D'Elia, H. Panagopoulos, and E. Vicari, Phys. Rev. Lett. **110**, 252003 (2013).
[54] C. Bonati, J. High Energy Phys. 03 (2015) 006.
[55] C. Bonati, M. D'Elia, and A. Scapellato, Phys. Rev. D **93**, 025028 (2016).
[56] K. Lawson and A. R. Zhitnitsky, Phys. Rev. D **95**, 063521 (2017).
[57] A. Zhitnitsky, arXiv:1707.03400.
[58] C. Cao and A. Zhitnitsky, Phys. Rev. D **96**, 015013 (2017).
[59] G. 't Hooft, Phys. Rev. D **14**, 3432 (1976).
[60] T. Schafer and E. V. Shuryak, Rev. Mod. Phys. **70**, 323 (1998).
[61] R. Rapp, T. Schfer, E. V. Shuryak, and M. Velkovsky, Ann. Phys. (N.Y.) **280**, 35 (2000).
[62] A. R. Zhitnitsky, Nucl. Phys. **A921**, 1 (2014).
[63] P. B. Arnold, G. D. Moore, and L. G. Yaffe, J. High Energy Phys. 11 (2000) 001.
[64] J.-W. Chen and E. Nakano, Phys. Lett. B **647**, 371 (2007).
[65] P. K. Kovtun, D. T. Son, and A. O. Starinets, Phys. Rev. Lett. **94**, 111601 (2005).